Cell Metabolism
Resource

Production of Functional Classical Brown Adipocytes from Human Pluripotent Stem Cells using Specific Hemopoietin Cocktail without Gene Transfer

Miwako Nishio,[1] Takeshi Yoneshiro,[4] Masako Nakahara,[1] Shinnosuke Suzuki,[1] Koichi Saeki,[5] Mamoru Hasegawa,[5] Yuko Kawai,[6] Hidenori Akutsu,[7] Akihiro Umezawa,[7] Kazuki Yasuda,[2] Kazuyuki Tobe,[8] Akira Yuo,[1] Kazuo Kubota,[3] Masayuki Saito,[9] and Kumiko Saeki[1,*]

[1]Department of Disease Control, Research Institute
[2]Department of Metabolic Disorder, Diabetes Research Center, Research Institute
[3]Department of Radiology
National Center for Global Health and Medicine, Tokyo 162-8655, Japan
[4]Laboratory of Histology and Cytology, Department of Anatomy, Hokkaido University Graduate School of Medicine, Sapporo 060-8638, Japan
[5]DNAVEC Corporation, Ibaraki 300-2511, Japan
[6]LSI Sapporo Clinic, Sapporo 065-0013, Japan
[7]Department of Reproductive Biology, Center for Regenerative Medicine, National Research Institute for Child Health and Development, Tokyo 157-8535, Japan
[8]The First Department of Internal Medicine, Faculty of Medicine, University of Toyama, Toyama 930-0194, Japan
[9]Department of Nutrition, School of Nursing and Nutrition, Tenshi College, Sapporo 065-0013, Japan
*Correspondence: saeki@ri.ncgm.go.jp
http://dx.doi.org/10.1016/j.cmet.2012.08.001

SUMMARY

Brown adipose tissue is attracting much attention due to its antiobestic effects; however, its development and involvement in metabolic improvement remain elusive. Here we established a method for a high-efficiency (>90%) differentiation of human pluripotent stem cells (hPSCs) into functional classical brown adipocytes (BAs) using specific hemopoietin cocktail (HC) without exogenous gene transfer. BAs were not generated without HC, and lack of a component of HC induced white adipocyte (WA) marker expressions. hPSC-derived BA (hPSCdBA) showed respiratory and thermogenic activation by β-adrenergic receptor (AdrRβ) stimuli and augmented lipid and glucose tolerance, whereas human multipotent stromal cell-derived WA (hMSCdWA) improved lipid but inhibited glucose metabolism. Cotransplantation of hPSCdBA normalized hMSCdWA-induced glucose intolerance. Surprisingly, hPSCdBAs expressed various hemopoietin genes, serving as stroma for myeloid progenitors. Moreover, AdrRβ stimuli enhanced recovery from chemotherapy-induced myelosuppression. Our study enhances our understanding of BA, identifying roles in metabolic and hemogenic regulation.

INTRODUCTION

Brown adipose tissue (BAT) is involved in nonshivering thermogenesis during cold exposure (Enerbäck et al., 1997) and diet-induced thermogenesis (Feldmann et al., 2009). It also contributes to the prevention of aging-associated obesity, as demonstrated in *Ucp1* null mice (Kontani et al., 2005). In large-sized mammals, the majority of BAT disappears within a few days after birth; however, some portions remain and function through adulthood. ^{18}Fluorodeoxyglucose-positron emission tomography in combination with computed tomography (^{18}F-FDG-PET/CT) along with histological and gene expressional studies has shown the presence of functional BAT in adult humans in supraclavicular and paravertebral regions (Cypess et al., 2009; Virtanen et al., 2009; van Marken Lichtenbelt et al., 2009; Saito et al., 2009; Yoneshiro et al., 2011). Although accumulating evidence has shown an inverse correlation between the amounts of active BAT and the development of metabolic syndrome in humans (Ouellet et al., 2011; Jacene et al., 2011), the cause-and-effect relationship between BAT and metabolic improvement remains unsubstantiated. Moreover, the whole picture of the development of human BAT is not clarified yet; for example, it remains elusive whether BAT derives from a common progenitor with myoblast, immature mesenchymal cells from which white adipocyte (WA) is also generated or from vascular components such as endothelial and perivascular cells (Tran et al., 2012; Gupta et al., 2012), and whether bone morphogenic protein 7 (BMP7) (Tseng et al., 2008) is sufficient or additional cytokines are required for BA differentiation. The newly proposed concept of brite adipocytes, WA-derived BA-like cells (*br*own + wh*ite* = brite) (Petrovic et al., 2010), makes the situation complex, often encumbering an understanding of classical BAT development. For an advanced understanding of BAT, establishing a method to generate BAs from pluripotent stem cells, including embryonic stem cells (ESCs) and induced pluripotent stem cells (iPSCs), is of great use. Recently, a trial to program human iPSCs (hiPSCs) into BA via transferring of exogenous genes was reported (Ahfeldt et al., 2012); however, biological effects of the programmed BA on lipid/glucose metabolism remains unevaluated. Moreover, artificially programmed

cells are not applicable to the investigations on natural developmental pathways of human BA.

The existence of BAT in bone marrow (BM), which attenuates with aging and diabetes, was reported in mice (Krings et al., 2012). Also, a nontumorous infiltration of BAT in human BM was reported in a case of essential hyperthrombocythemia (Thorns et al., 2008). A functional link between BM fat and hematopoiesis was first reported by Dexter et al. (Dexter et al., 1977), who showed that BM adipocytes with mitochondria-attached multilocular lipid droplets were essential for the maintenance of colony-forming units-spleen (CFU-S), a short-term repopulating hematopoietic progenitor cell (HPC) distinct from hematopoietic stem cell (HSC). Although the microenvironment for HSC (reviewed in Kiel and Morrison, 2006; Arai and Suda, 2007) and B cells (Nagasawa, 2007) has been intensively studied, that for myeloid progenitor cells (MPCs) remains poorly understood. Moreover, controversial findings have been reported regarding the effects of "BM adipocyte" on the committed HPCs: some reports showed its capacity to support lymphopoiesis (Gimble et al., 1990) and granulopoiesis (Gimble et al., 1992), while others showed its inhibiting effects for hematopoiesis (Ookura et al., 2007, Naveiras et al., 2009). The controversy may come from, at least in part, the heterogeneity of bone marrow fat cells including BAT versus white adipocyte tissue (WAT).

During our research into the feeder-free hematopoietic differentiation of hPSCs, we serendipitously found the existence of BA-like cell clusters surrounding the hematopoietic centers and an induction of BA-selective gene, *PRDM16* (see Figure S1 online). Because the hematopoietic differentiation was achieved under a completely feeder-free condition, a de novo hematopoietic stroma must be generated from hPSCs per se. Eventually, murine C3H10T1/2 line, a commonly used feeder for the hematopoietic differentiation of monkey (Hiroyama et al., 2006) and human (Takayama et al., 2008) ESCs, can differentiate into functional BA (Tseng et al., 2008). Thus, an association between BA development and hemopoiesis has been suggested.

After a process of trial and error, we established a high-efficiency method to produce functional BAs from hPSCs including human ESCs (hESCs) and hiPSCs. Involvement of hPSC-derived BAs (hPSCdBAs) in metabolic improvement, its service as a stroma for MPCs, and the existence of BA in vertebral BM are also shown.

RESULTS

Directed Differentiation of Human PSC into Functional BA

By utilizing a specific hemopoietin cocktail (HC) composed of KIT ligand (KITLG), fms-related tyrosine kinase 3 ligand (FLT3LG), interleukin-6 (IL-6), and vascular endothelial growth factor (VEGF) along with the previously reported BA inducer BMP7 (Tseng et al., 2008), we successfully established a highly efficient BA differentiation method for hESCs and hiPSCs (Supplemental Information). The differentiated cells exclusively contained multilocular lipid droplets (Figure 1A), as confirmed by oil red O staining (Figure 1B). Quantitative RT-PCR studies demonstrated the induction of BAT-specific genes of *UCP1* and *PRDM16*, which were not detected in human multipoint stromal cell-derived WA (hMSCdWA) (Figure 1C). Although depletion of BMP7 significantly lowered BA differentiation efficiency as reported by Tseng et al. (Tseng et al., 2008) (Figure S2), BA differentiation was completely abolished by HC depletion even in the presence of BMP7 (Figure 1D). Expression of a series of BAT-selective and BAT/WAT-common genes, but not WAT-selective genes, was also determined (Figure 1E). UCP1 protein expression was confirmed by immunostaining studies, showing that over 95% of the BA differentiated cells expressed UCP1 at mitochondria (Figure 2A), and also western blotting, showing the presence of a 32 kDa band in the differentiated cells (Figure 2B). Lipid staining illustrated the wide distribution of mitochondria within the cytosol, some of which resided close to lipid droplets (Figure 2C). Electron micrographs confirmed the presence of multilocular lipid droplets and abundant mitochondria rich in transverse cristae (Figure 2D and Figure S3A), some of which located in close vicinity to lipid droplets (Figure S3B), in contrast to hMSCdWA, which showed meager mitochondria (Figure S3C).

We next evaluated the functional maturation of hESC/hiPSC-derived BAs. First, thermogenic potential was evaluated. Treatment with a β-adrenergic receptor, isoproterenol, augmented the expression of *UCP1*, a major contributor to thermogenesis, and *PRDM16*, a major inducer of *UCP1* expression, in hPSCdBAs (Figures 3A and 3B, left). Isoproterenol-responsive thermogenic activation (Jackson et al., 2001) was further confirmed in vivo by subcutaneous transplantation of hPSCdBAs into mice (Figures 3A and 3B, right). Respiratory activation was also assessed in vitro: hPSCdBAs showed considerably higher basal and maximum OCRs than hMSCdWA as demonstrated by a standard Mito Stress Test (Figure 3C). Responsiveness to a β3-adrenergic receptor-selective agonist, CL316,243, was also determined: statistically significant upregulation in oxygen consumption rates (OCRs) was determined in the cases of hPSCdBAs in response to CL316,243, whereas no significant changes were observed in the cases of hMSCdWA and immature hPSCs (Figure 3D). Upregulation of OCR was further determined in isoproterenol-treated hPSCdBAs (data not shown).

Together, these findings support the production of functional BAs from hPSCs.

Effects of hPSC-Derived BA on Lipid and Glucose Metabolism

Because endogenous BAT reportedly reduces blood triglyceride (TG) levels in response to cold stimuli (Bartelt et al., 2011), we examined the effects of transplantation of hPSCdBA on lipid metabolism. Compared to immature hPSC-transplanted mice, hPSCdBA-transplanted mice (Figure 4A, middle column) and hMSCdWA-transplanted mice (Figure 4A, right column) showed reduced fasting TG levels. Olive oil tolerance tests further confirmed that hPSCdBA transplantation augmented resistance to oral lipid loading (Figure 4B).

Next, effects of hPSCdBAs on glucose metabolism were evaluated. Ten-week-old mice were subcutaneously injected with saline, hESC-derived BA (hESCdBA), or hMSCdWA, and blood glucose levels were measured over time (Figure 4C). Fasting blood glucose levels were significantly lowered in hESCdBA-transplanted mice compared to saline-injected mice ($p = 0.0032$; $n = 3$) and to hMSCdWA-transplanted mice ($p = 0.0030$;

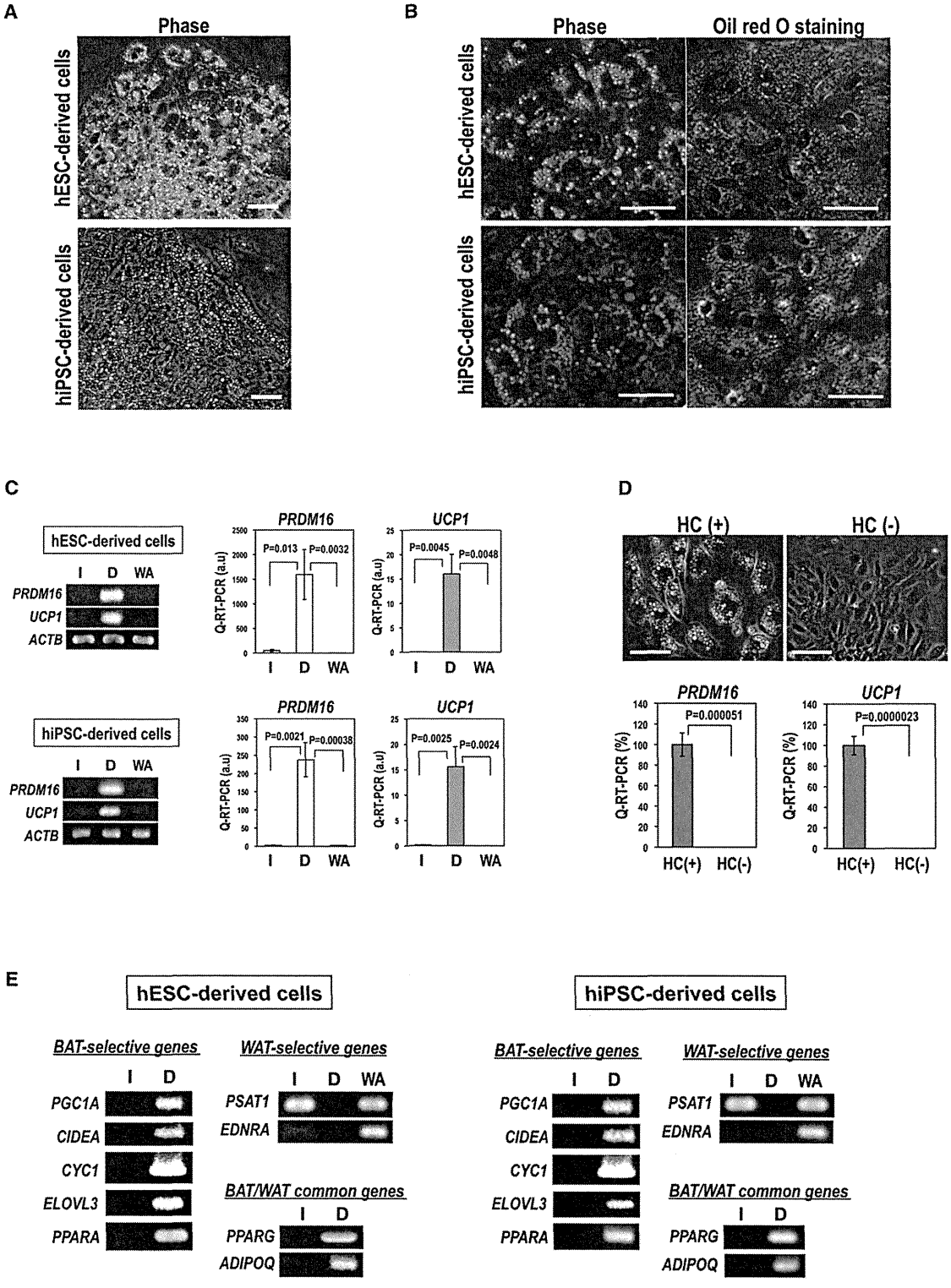

Figure 1. Differentiation of hPSCs into BAs

(A) Microscopy of hPSC-derived cells. Scale bar, 50 μm.

(B) Oil red O staining (right) with phase contrast microscopy (left). Scale bar, 40 μm.

(C) Expression of *PRDM16* and *UCP1* determined by RT-PCR (left) or real-time PCR (middle and right). The error bars represent average ± standard deviation (SD) (n = 3).

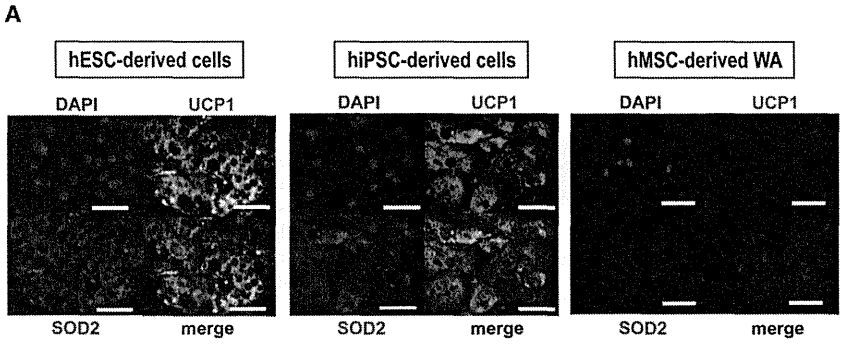

Figure 2. Analyses on Protein Expressions and Fine Structures

(A) Immunostaining using an anti-UCP1 and anti-SOD2 antibody as indicated. Scale bar, 50 μm.

(B) Western blotting using an anti-UCP1 as indicated.

(C) Lipid staining. hESC-derived differentiated cells were stained by an anti-UCP1 antibody (red) and BODIPY 493/503 (green). Scale bar, 5 μm.

(D) EM of hiPSC-derived cells (left) and hESC-derived cells (right). L, lipid droplets; M, mitochondria. Scale bar, 2 μm.

(data not shown), confirming that hMSCdWA transplantation deteriorates glucose metabolism. The different effects between hESCdBA and hMSCdWA were not due to the difference in cell survival, as we clearly detected the existence of transplanted cells (Figure S4A). Moreover, deterioration of glucose metabolism by hMSCdWA transplantation could not be attributed to inflammation, because we did not observe any signs of inflammation, such as macrophage infiltration (Figure S4B). In addition, hMSCdWA did not express tumor necrosis factor α (*TNFA*), and it expressed only a low level of *IL1B* (Figure S4C).

We also examined longer-term effects of hPSCdBA transplantation using immunocompromised NOG mice (Ito et al., 2002). Fasting blood glucose level-lowering effects of hESCdBA were determined at least for 3 weeks (Figure 4G). Cells with multilocular lipid droplet (Figure 4H) that expressed UCP1 (Figure 4I) and human HLA-A,B,C (Figure 4J) were determined by histological analyses. Around the graft tissue, microvasculatures were also detected (Figure 4H arrowheads).

n = 3) (Figure 4D). Surprisingly, hMSCdWA-transplanted mice showed elevated homeostasis model assessment-insulin resistance (HOMA-IR) values compared not only with hESCdBA-transplanted mice ($p = 0.0003$; $n = 3$) but also with saline-injected mice ($p = 0.0011$; $n = 3$) (Figure 4E), indicating that hMSCdWA induces insulin resistance despite its favorable effect on lipid metabolism. Similar results were obtained when 6-week-old younger mice were used for the assay (data not shown). As shown in Figure 4F, oral glucose tolerance tests (OGTTs) further demonstrated that hESCdBA transplantation reduced 15 min blood glucose values compared to saline injected ($p = 0.010$; $n = 3$), while hMSCdWA-transplanted mice exhibited elevated 30 min blood glucose values compared not only with hESCdBA-transplanted mice ($p = 0.0034$; $n = 3$) but also with saline-injected mice ($p = 0.0055$; $n = 3$). Similar results were obtained when 6-week-old younger mice were used for the assay

Finally, we assessed possible therapeutic effect of hESCdBA on hMSCdWA-induced deterioration of glucose metabolism. Although no significant changes in fasting blood glucose values and HOMA-IR values were observed (Figure 4K and 4L), cotransplantation of an equivalent number of hESCdBA ameliorated the deleterious effect of hMSCdWA, significantly lowering the 30 min blood glucose values ($p = 0.0014$; $n = 3$) (Figure 4M).

All those findings together indicate that (1) hPSCdBAs improve both lipid and glucose metabolism, (2) hMSCdWA improved lipid but deteriorates glucose metabolism, and (3) hPSCdBAs ameliorate adverse effects of hMSCdWA on glucose metabolism.

(D) BA differentiation in the presence or absence of HC. Microscopy (upper) and expressions of *PRDM16* (lower left) and *UCP-1* (lower right) by real time PCR were shown. Scale bar, 50 μm. The error bars represent average ± SD ($n = 3$).

(E) Expression of BAT-selective, BAT/WAT-common, and WAT-selective genes examined by RT-PCR. I, immature hPSC; D, differentiated hPSC; WA, hMSCdWA.

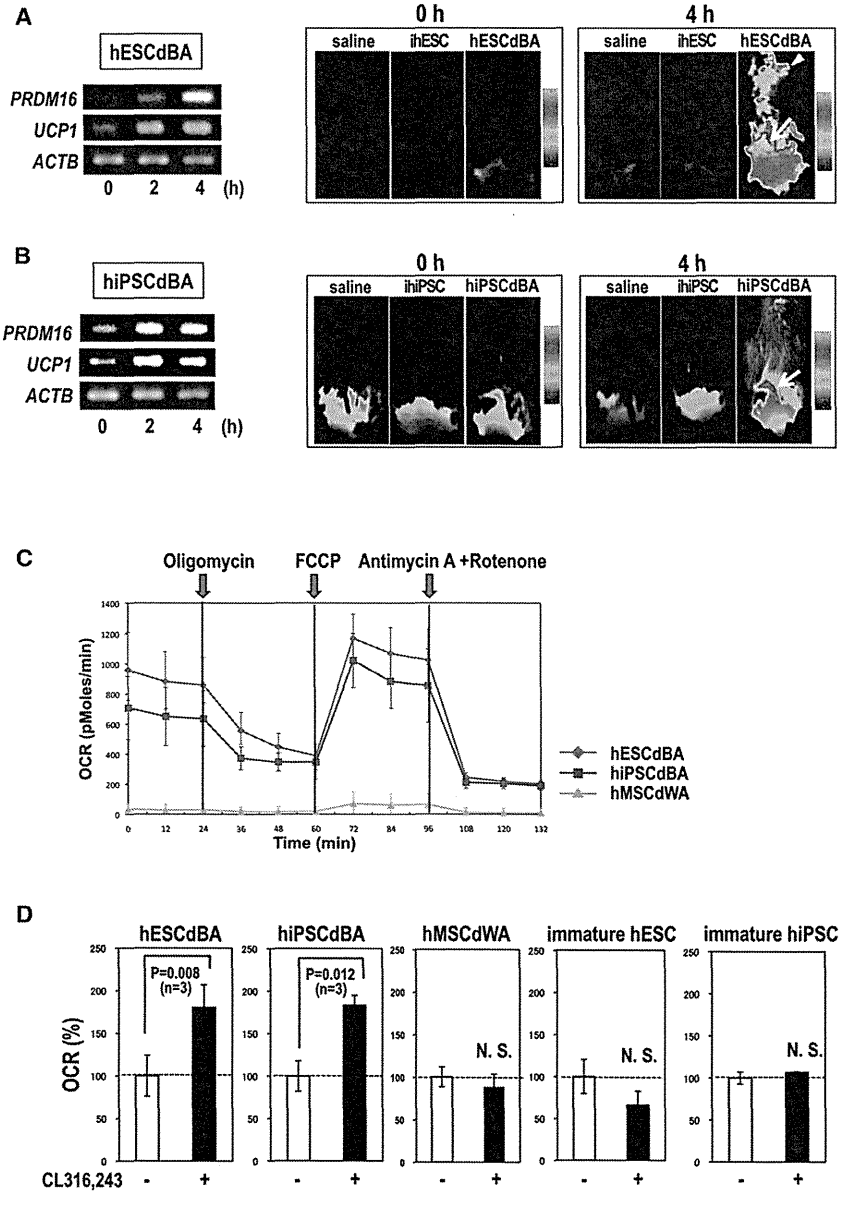

Figure 3. Thermogenic and Mitochondrial Respiratory Activation

(A and B) Thermogenesis studies. hESCdBA (A) and hiPSCdBA (B) were treated with isoproterenol. Gene expression was examined by RT-PCR over time (A, left; B, left). Thermographic images of mice transplanted with saline, immature hESC (ihESC), hESCdBA, immature hiPSC (ihiPSC), or hiPSCdBA before and after isoproterenol treatments are shown (A, right; B, right). Arrows indicate regions of transplantation; arrowheads indicate areas of endogenous murine BAT.

(C) Mito stress tests were performed using hESCdBA, hiPSCdBA, and hMSCdWA as indicated.

(D) OCR was measured in hESCdBA, hiPSCdBA, hMSCdWA, immature hESCs, and immature hiPSCs after a 4 hr incubation with or without CL316,243. The error bars in (C) and (D) represent average ± SD (n = 3).

ment (Figure 5B). Thus, our method correctly mimics the classical BAT development but not a brite adipocyte pathway via immature mesenchymal stem cell differentiation.

We further evaluated the detailed role of each hematopoietin. The absence of any one of the components of HC lowered the quality of BA differentiation, reducing cellular viability and/or percentages of multilocular lipid-containing cells (Figure 5C). Gene expression studies further showed that VEGF was required for *PRDM16* expression, whereas KITLG, IL6, or FLT3LG was required for subsequent *UCP1* expression (Figure 5D). Surprisingly, depletion of either KITLG, IL6, or FLT3LG paradoxically induced the expression of a WAT marker, phosphoserine aminotransferase 1 (*PSAT1*) (Seale et al., 2007), and a lateral plate mesoderm marker, vegfr2. Thus, the HC is essential for the differentiation of hPSCs into classical BA, and the omission of any of the HC components results in WAT lineage commitment.

Signaling for BA Differentiation

To confirm that our differentiation technique correctly reproduced classical BAT development via myoblastic differentiation (Timmons et al., 2007; Seale et al., 2008; Sun et al., 2011), the expression of a series of developmental markers was examined. As shown in Figure 5A, myoblastic *MYF5* expression was transiently upregulated during the initial floating culture step of differentiation. Moreover, the expression of a paraxial mesoderm marker, platelet-derived growth factor receptor α (*PDGFRA*) (Sakurai et al., 2006), was upregulated. By contrast, the levels of immature mesenchymal stem cell marker, *NG2* and *PDGFRB* (Crisan et al., 2008), as well as a lateral plate mesoderm marker, VEGFR2 (Sakurai et al., 2006), were reduced. The precedence of myoblastic differentiation was further confirmed by the transient induction of PAX3/7, which are involved in myogenic commit-

We also examined intracellular signaling by performing inhibitor analyses. Because a BMPR1a inhibitor (BMPR1a-i) and p38 MAPK inhibitor (p38-i) reportedly hamper BA differentiation (Sellayah et al., 2011), effects of these two inhibitors, along with those of a MAP kinase-ERK kinase (MEK) inhibitor (MEK-i), were examined. We found that BMPR1a-i induced massive cell death during the floating culture step of BA differentiation (Figure 5E, second left). Cell death had been induced as early as day 1 (data not shown). Similar results were obtained from the case of AKT inhibitor (AKT-i). (Figure 5E, right). Thus, BMPR1a-dependent signaling is required for the survival of immature sphere-forming progenitor cells, from which mature BA will be produced. We then followed up the p38-i- and MEK-i-treated

cells until day 10, when mature BA was generated. In the case of hESC, p38-i treatment reduced the number of lipid droplet-containing cells (Figure 5F, upper middle), while MEK-i treatment exerted minimal effects (Figure 5F, upper right). Compatible to these morphological findings, p38-i treatment, but not MEK-i treatment, lowered *PRDM16* and *UCP1* expression levels (Figure 5G, left half). By contrast, p38-i treatment exerted minimal effects on hiPSCs (Figure 5F, lower middle), whereas MEK-i treatment induced cogeneration of the cells with unilocular lipid droplets (Figure 5F, lower right). Compatibly, *PRDM16* and *UCP1* expressions were only slightly reduced in p38-i-treated hiPSCs but clearly reduced in MEK-treated hiPSCs (Figure 5G, right half). Therefore, p38 MAPK and ERK signaling play important roles in BA differentiation depending on the lines or kinds of hPSCs.

A Functional Link between BA and Hematopoiesis

There has been a controversy regarding the effect of BM adipocytes on the proliferation and differentiation of committed HPCs. For example, murine BM adipocytic lines are reportedly capable of supporting lymphopoiesis (Gimble et al., 1990) and granulopoiesis (Gimble et al., 1992), whereas human BM-derived fat cells generated by a dexamethasone/insulin treatment reduce colony-forming capacities of HPCs (Ookura et al., 2007). We hypothesized that the controversy came from the heterogeneity of BM adipocytes and that BA, but not WA, serves as a stroma for committed HPCs for the following reasons: (1) hematopoietic stromal cells essential for maintaining CFU-S exhibit morphological resemblance to BA rather than to WA (Dexter et al., 1977); (2) the murine embryo-derived C3H10T1/2 cell line (Reznikoff et al., 1973), which differentiates into mature BAT on BMP7 treatment (Tseng et al., 2008), is widely used as a feeder for the hematopoietic differentiation of monkey (Hiroyama et al., 2006) and human (Takayama et al., 2008) ESCs; (3) BM is replaced by WA in severe myelosuppressive states including aplastic anemia; and (4) treatment with dexamethasone/insulin induces differentiation into WA but not BA.

To validate our hypothesis, human umbilical cord blood $CD34^+$ HPCs were cultured on hESCdBA layers for 1 week in the absence of any recombinant hematopoietic cytokines. Then, floating cells were subjected to intrabone marrow transplantation (IBM-T) into alymphocytic NOG mice, and after 8 weeks, splenic chimerisms were measured to assess the expansion of CFU-S. For a control, $CD34^+$ cells were directly transplanted without culturing on hPSCdBA layers (Figure 6A). As shown in Figure 6B, splenic chimerisms were significantly higher in hPSCdBA-cocultured $CD34^+$-transplanted mice than in mice with direct transplantation ($p = 0.041$; $n = 3$). Moreover, percentages of human CD33-positive myeloid cells were larger in cocultured $CD34^+$-transplanted mice (4.8 ± 0.13 versus 3.0 ± 0.19; $p = 0.00022$; $n = 3$, data not shown), while no significant changes in B lymphocyte percentages were observed (data not shown). These findings indicate that hPSCdBA serves as a stroma for MPCs, promoting their expansion/differentiation and homing to the spleen.

We also examined the expression of hematopoietic cytokines involved in the expansion and differentiation of committed HPCs. Various hematopoietin genes including thrombopoietin (*THPO*), *IL6*, *IL3*, colony-stimulating factor 3 (*CSF3*), colony-stimulating factor 2 (*CSF2*), and erythropoietin (*EPO*) were expressed in hESCdBA (Figure 6C, middle lanes) and hiPSCdWA (data not shown). On the other hand, hMSCdWAs expressed only *IL6* among these hemopoietins (Figure 6C, right lanes). Moreover, the expression levels of the hematopoietin genes in hESCdBA (Figure 6D) and hiPSCdBA (data not shown) were upregulated by isoproterenol treatments, further supporting the notion that hPSCdBA serves as stromal for committed HPCs.

To evaluate in vivo relevance, we examined whether isoproterenol treatment could enhance the recovery from antitumor agent-induced myelosuppression by enhancing the expansion/differentiation of MPCs. Mice were treated with 5-fluorouracile (5-FU), and bone marrow cells were collected and analyzed over time (Figure 6E). As reported by Hofer et al. (Hofer et al., 2007), 5-FU-treated mice were at the nadir at day 3, when a decline in total enucleated cell number (11.33 ± 1.74 versus 4.87 ± 0.96 [$\times 10^6$], $p = 0.0023$; $n = 3$) (Figure 6F) as well as a reduction in early myeloid cells (Figures S5A–S5C) were observed. Although total cell number (8.70 ± 0.40; $n = 3$) (Figure 6F) and the percentages of R1 fraction (Figures S5A and S5B) were eventually upregulated at day 7 as a sign of a recovery from myelosuppression, the mice still suffered from a shortage of mature myeloid cells (Figures S5A–S5C). By contrast, isoproterenol-treated mice showed higher enucleated cell number (10.93 ± 1.14, $p = 0.032$; $n = 3$) (Figure 6F) with significantly larger R2 fraction percentages (Figures S5A and S5B). Cytological studies confirmed all those findings (Figure S5C).

The existence of BA in BM has long been suggested despite the lack of direct evidence (reviewed in Motyl and Rosen, 2011). A relationship between osteoblast and BA was reported in mice (Calo et al., 2010). Moreover, murine BM fat reportedly expresses various BA-selective messages (Krings et al., 2012). To assess the possible existence of BA in human BM, expressions of BAT-specific markers, *UCP1* and *PRDM16*, were examined using commercially available human BM RNA samples. As shown in Figure 7A, expression of both genes was detected by RT-PCR, whereas they were undetectable in human BM-originated MSC-derived WA (hBM-MSCdWA). To further assess the existence of active BM-BAT in vivo, ^{18}F-FDG-PET/CT examinations were performed in healthy young volunteers (24.8 ± 5.8 of age; $n = 20$) with or without cold stimuli (Saito et al., 2009; Yoneshiro et al., 2011). We identified cold-stimulated ^{18}F-FDG uptake in vertebral BM (Figures 7B–7D), whose signal intensities showed an intimate correlation with those of BATs ($p < 0.001$), but not of those of brain, heart, spleen, or muscle (Figures S6A and S6B). The presence of vertebral BM was histologically examined using 3-week-old murine vertebral BM samples: we successfully detected the cells with BA morphologies (Figure 7E) that were positive for UCP1 protein expression (Figure 7F). Collectively, those findings strongly suggest the presence of functional BA in the BM of vertebrae.

DISCUSSION

We established a highly efficient method for the differentiation of hPSCs into functional BAs. This is the first success in generating functional classical BA pluripotent stem cells without exogenous gene transfer. By virtue of its technological merits, our method provides a valuable tool for BAT research. Functional

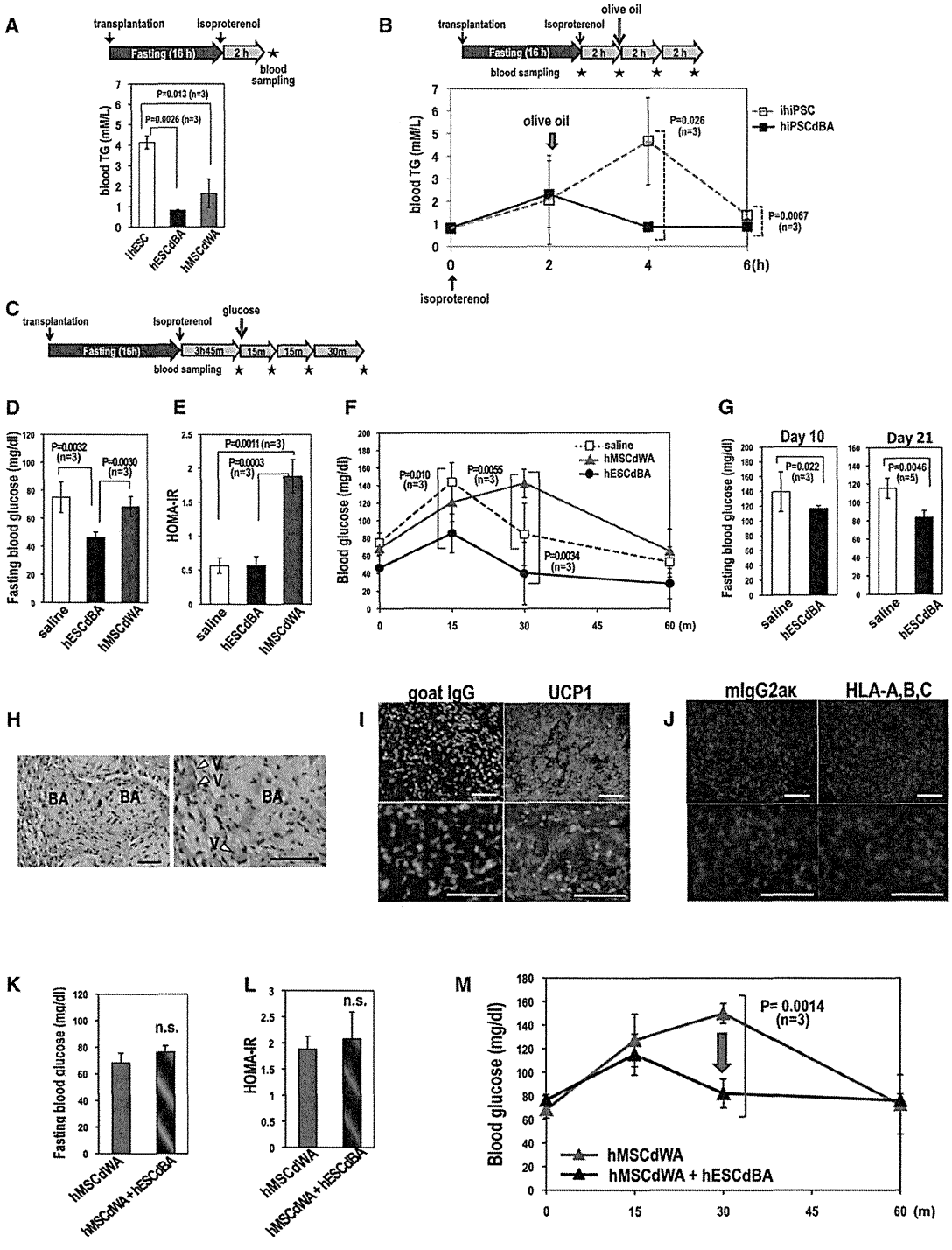

Figure 4. Metabolic Improvement by hPSC-Derived BA Transplantation

(A) Blood TG clearance tests. Immunocompetent ICR mice were transplanted with immature hESCs (ihESC) (n = 3 mice), hESCdBA (n = 3 mice), or hMSCdWA (n = 3 mice). After 16 hr starvation, isoproterenol was administrated and blood TG levels were measured.

(B) Oral fat tolerance tests. ICR mice were transplanted with immature hiPSC (ihiPSC) (n = 3 mice) or hiPSCdBA (n = 3 mice). Olive oil was orally loaded, and blood TG levels were measured over time after isoproterenol treatments.

(C–F) OGTT. ICR mice were injected with saline (n = 3 mice), hESCdBA (n = 3 mice), or hMSCdWA (n = 3 mice), and OGTT was performed (C). Fasting blood glucose levels (D), HOMA-IR (E), and blood glucose values after oral glucose loading (F) are shown.

(G–J) Immunocompromized NOG mice were injected with saline or transplanted with hESCdBA. At indicated time points, fasting blood glucose levels were measured. Three mice (day 10) or five mice (Day 21) were used for each condition (G). Histological studies were performed by HE staining (H) and

BA, which is responsible to a β3-adrenergic receptor agonist, has also been generated from human multipotent adipose-derived stem cells by chronic treatment with thiazolidinediones (Elabd et al., 2009). The merit of our system is that it does not require preparation of human specimen materials but utilizes hPSCs, which are capable of unlimited expansion in vitro.

One of the main findings of our research is that HC composed of KITLG, IL6, FLT3LG, and VEGF is essential for BA differentiation of hPSCs. Although BMP7 plays an important role in BA differentiation of hPSC (Figure S2) as reported in murine cases (Tseng et al., 2008), HC is indispensable for BA differentiation of hPSCs (Figure 1D). It is known that VEGF is synthesized in rodent BAT (Asano et al., 1997; Tonello et al., 1999), promoting the angiogenesis within BAT. Moreover, IL6 is reportedly secreted from cultured human BM adipocytes (Laharrague et al., 2000). Our findings imply that VEGF and IL6, together with KITLG and FLT3LG, work as fundamental autocrine or paracrine factors to promote BA differentiation.

Compatible to the finding by Sellayah et al. (Sellayah et al., 2011), the inhibitor analyses demonstrated the involvement of p38 MAPK signaling, but not of MEK signaling, in BA differentiation of hESC (Figures 5E–5G). However, distinct findings were obtained from the case of hiPSCs, in which MEK signaling played a role in BA differentiation (Figure 5E–5G). At this moment, the basis for the difference in the effects of identical inhibitors between hESCs and hiPSCs remains elusive. It may be related to the difference in the genetic background of pluripotent stem cell lines, reflecting the individual difference of the "donor" or the difference in the type of pluripotent stem cells or both. Further investigations are required to obtain the whole picture of the molecular basis for BA differentiation of hPSCs.

By providing high-purity human BA and WA materials, we demonstrated the differential effects on metabolic regulation between BA and WA: BA improves while WA deteriorates glucose metabolism. Because those effects were confirmed by a short-term assay without body weight changes and also because the effects of BA and WA on lipid metabolism were similar, the beneficial effect of BA on glucose metabolism is not a secondary consequence of general metabolic improvement. Conventional subcutaneous fat transplantation experiments were not able to distinguish the effect of BA from that of WA, because subcutaneous fat tissues contain both WA and BA. Thus, our system will provide a unique tool for the research of BA in regard to glucose metabolism.

Another surprising finding is the functional link between BA and hematopoiesis. We showed that hPSCdBAs serve as a stroma for MPCs. In contrast to the "niche" for HSCs, which is composed of immature osteoblasts and sinusoidal endothelial cells, the "stroma" for committed HPCs remains a mystery. The only report showing the characteristic of such stroma was a study by Dexter et al. (Dexter et al., 1977), in which BM fat cells with multilocular lipid droplets attached by mitochondria were identified as a stroma for CFU-S. Our results indicating that (1) hPSCdBAs express various hematopoietic cytokines in response to β-adrenergic receptor stimuli, (2) hPSCdBAs promote myelopoiesis of human cord blood $CD34^+$ cells, and (3) β-adrenergic receptor stimuli accelerate the recovery from 5-FU-mediated myelosuppression together show that BM-BAT serves as a stroma for MPCs. Among those, the third finding is particularly important because it illustrates a very feasible way to shorten the period of myelosuppression, the major side effect of intensive chemotherapy for progressive cancers.

The PET-CT results of young healthy volunteers, together with gene expression analyses of human BM specimen and histological examinations of murine vertebral BM samples, strongly suggest the existence of active BAT in vertebral BM in mammals. Because classical BAT is derived from *Myf5*-positive myoblastic cells (Seale et al., 2008) and because *Myf5*-positive cells emerge at the juxtaspinal, prospectively paravertebral, regions within somites (Cossu et al., 1996; Braun and Arnold, 1996), the existence of BA in vertebral BM seems reasonable. Because the major portions of vertebrae are composed of trabecular bones, which are the sites of active hematopoiesis, and the vertebral marrow is the last reserve site for hematopoietic activity in aged individuals (Tanaka and Inoue, 1976), the hematopoietic microenvironment of vertebral BM may bear a unique character. Further investigation will elucidate the whole picture of HPC regulation.

Our system, providing highly functional hiPSCdBA, may open a new avenue to the therapy for obesity. However, we have found that BA differentiation efficiencies substantially differ among hiPSC lines (data not shown), as reported in the case of pancreatic β cell differentiation of hESCs (Osafune et al., 2008). For clinical application, selection of appropriate lines of hiPSCs will be as important as sophisticating the whole differentiation process into good manufacturing practice levels.

EXPERIMENTAL PROCEDURES

Establishment of hiPSCs and Provision of hESCs

SeV-iPS cells were established from human neonatal fibroblast or human umbilical vein endothelial cells by introducing Yamanaka's four factors using CytoTune-iPS ver.1.0 (DNAVEC Corp) (Figure S7). Transgenes were eliminated by a 39þC heat treatment for 5 days. A hESC line (KhES-3) was generously provided by the Institute for Frontier Medical Science, Kyoto University (Suemori et al., 2006).

A Directed Differentiation of hESCs/hiPSCs into Functional BA

hESCs or hiPSCs were cultured in a 6 cm low-attachment culture dish using a serum-free differentiation medium composed of 1:1 ratio of IMDM (I3390, Sigma Chemical Co.) and Ham's F12 (087-08335, WAKO Pure Chemical Industries), 5 mg/ml bovine serum albumin (A802, Sigma Chemical Co.), 1:100 synthetic lipids (GIBCO #11905-031, Life Technologies, Inc.), 450 μM α- monothioglycerol (207-09232, WAKO Pure Chemical Industries), 1:100 insulin-transferrin-selenium (ITS-A, Life Technologies, Inc.), 2 mM Glutamax II (GIBCO #35050-061, Life Technologies, Inc.), 5% protein-free hybridoma mix (PFHMII, GIBCO #12040-077, Life Technologies, Inc.), 50 μg/ml ascorbic acid-2-phosphate (Sigma, A-8960), and the hematopoietic cytokine cocktail I (5 ng/ml IGF-II, 20 ng/ml BMP4, 5 ng/ml VEGFA, 20 ng/ml KITLG, 2.5 ng/ml FLT3LG, 2.5 ng/ml IL-6) for 8 days to form spheres. The

immunostaining using an anti-UCP1 antibody (I) and anti-human HLA-A,B,C antibody (J) at day 7. Arrowheads in (H) indicate microvasculatures. Scale bars, 50 μm.

(K–M) Mice were transplanted with hMSCdWAs alone or together with hESCdBA, and OGTT was performed. Fasting blood glucose levels (K), HOMA-IR (L), and blood glucose values after oral glucose loading (M) are shown. The error bars in (A), (B), (D)–(G), (K), (L), and (M) represent average ± SD.

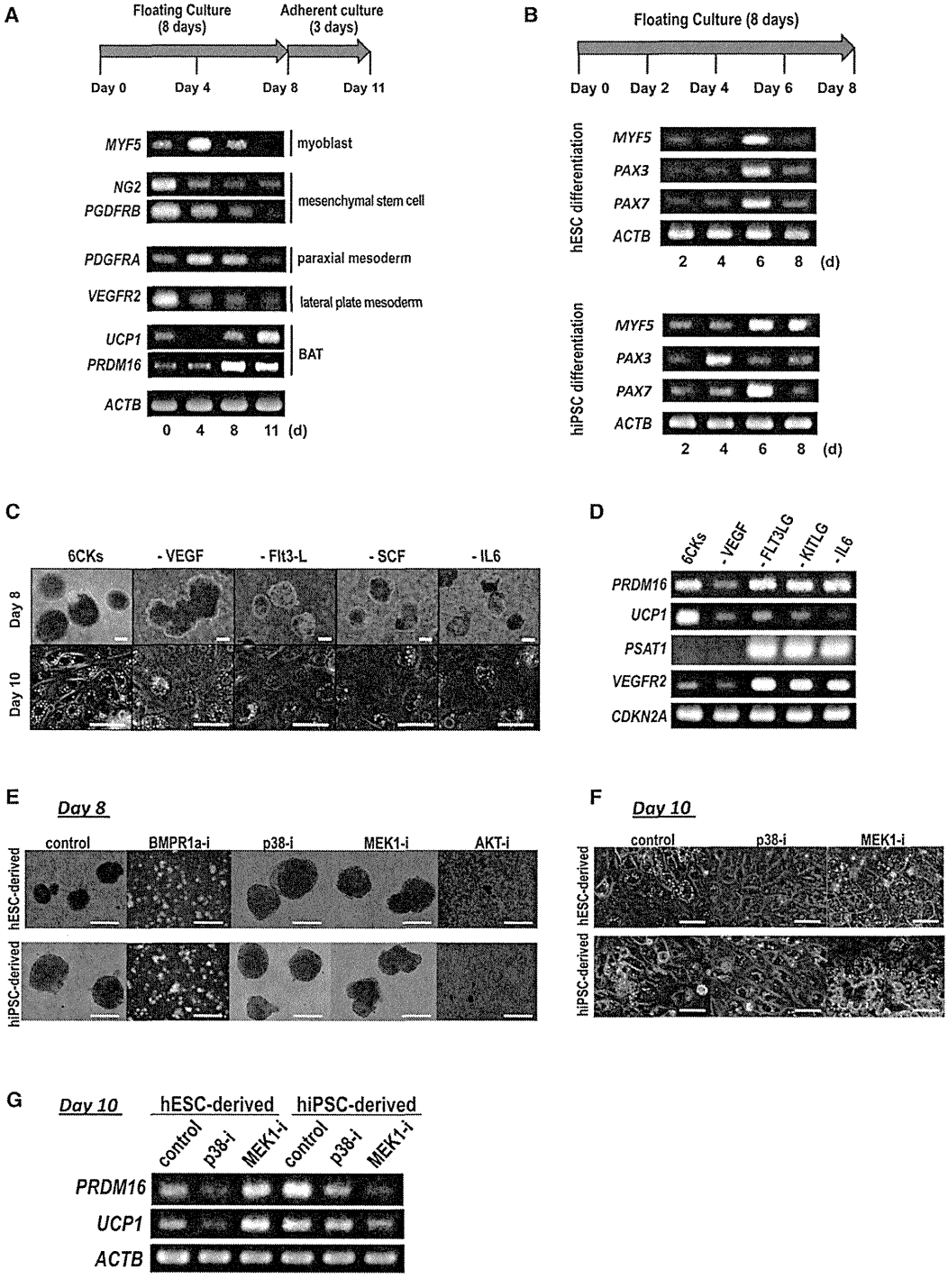

Figure 5. Signals Involved in BA Differentiation

(A) Developmental marker expression was examined by RT-PCR during BA differentiation of hESCs. Similar results were obtained regarding hiPSCs (data not shown).

(B) Myoblastic marker expressions were determined by RT-PCR during floating culture.

(C and D) The role of each cytokine was evaluated by morphological examinations (C) and RT-PCR (D). Scale bar, 100 μm (upper panels); and scale bar, 150 μm (lower panels).

(E–G) Inhibitor analyses. BA differentiation was performed in the presence of inhibitors of BMPR1a, p38 MAPK, MEK1, or AKT as indicated. Phase contrast micrographs of the spheres at day 8 (scale bar, 200 μm) (E) and those of BA at day 10 (scale bar, 50 μm) (F) were shown. Expressions of *UCP1* and *PRDM16* were determined at day 10 by RT-PCR (G).

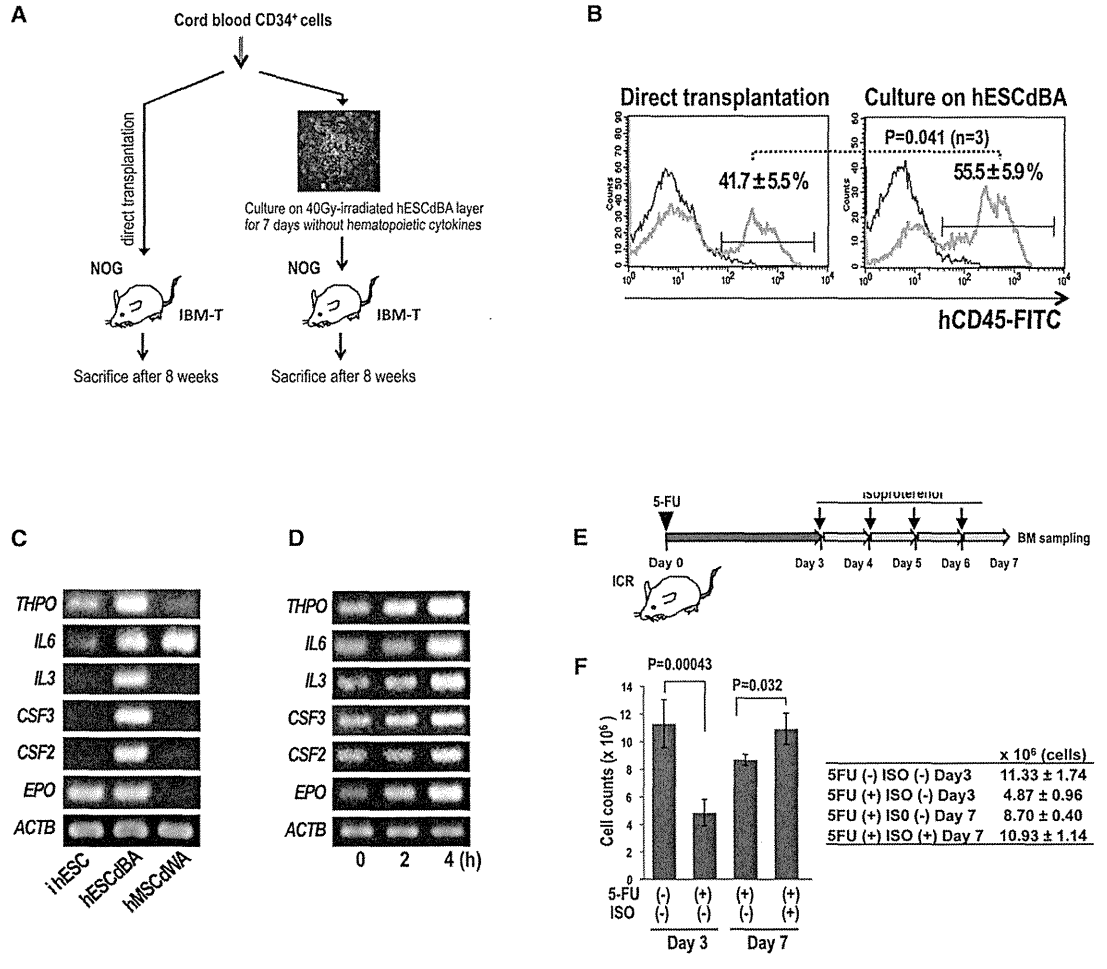

Figure 6. Hematopoietic Stromal Assays

(A) Schematic presentation of the assay.

(B) After 8 weeks from transplantation, cells were collected from the spleen and subjected to flow cytometry. hCD45-positive percentages were calculated. Similar results were obtained at 6 and 12 weeks after transplantation (data not shown). The error bars represent average ± SD (n = 3).

(C and D) Various hematopoietin expression was examined by RT-PCR in immature hESCs (ihESCs), hESCdBAs, and hMSCdWAs (C). Hematopoietin expression in hESCdBAs after isoproterenol treatments was examined over time by RT-PCR (D).

(E and F) 5-FU treatment assay. Experimental procedure (E) and the results of BM-enucleated cell counts (F) were shown. The error bars represent average ± SD (n = 3).

hESC/hiPSC-derived spheres were further cultured on gelatin-coated 6-well plates using the above-described serum-free medium supplemented with the hematopoietic cytokine cocktail II (5 ng/ml IGF-II, 10 ng/ml BMP7, 5 ng/ml VEGFA, 20 ng/ml KITLG, 2.5 ng/ml FLT3LG, 2.5 ng/ml IL-6) for several days.

Protein Expression Analyses

Immunostaining was performed using a goat polyclonal anti-human UCP1 antibody (sc-6528, Santa Cruz Biotechnology, Inc.) or a rabbit polyclonal anti-human SOD2 antibody LS-C39331, LifeSpan BioSciences Inc., Seattle, WA) as described previously (Nakahara et al., 2009). Western blotting was performed using a rabbit polyclonal UCP1 (Ab10983) (Abcam plc., Cambridge, UK) as described previously (Nakahara et al., 2009).

Gene Expression Analyses

RT-PCR was performed using primers described in Supplemental Information. Quantitative RT-PCR (qPCR) was performed by applying SYBR Green qPCR method using primers purchased from SuperArray (QIAGEN Science, Maryland, USA) as described in the Supplemental Experimental Procedures. The results were normalized by *GAPDH*.

Electron Microscopic Examinations

Cells were fixed by 2.5% glutaraldehyde. Postfixation by 2% osmium tetroxide, along with sample embedding into resin and slicing, was performed by Bio Medical Laboratories Co. Ltd. (Tokyo, Japan) (Saeki et al., 2000).

Inhibitor Analyses

BA differentiation was performed by adding the following inhibitors to the differentiation medium: 10 μM p38 MAP kinase inhibitor (Cat 506126) (Calbiochem Co., Darmstadt, Germany), 50 μM MEK1 inhibitor (PD 98059) (Calbiochem Co.), 10 μM BMPR1a inhibitor (Dorsomorphin Dihydrochloride, Cat 047-31801) (WAKO Pure Chemical Industries, Osaka, Japan), and 10 μM Akt inhibitor IV (Cat 124011) (Calbiochem Co.).

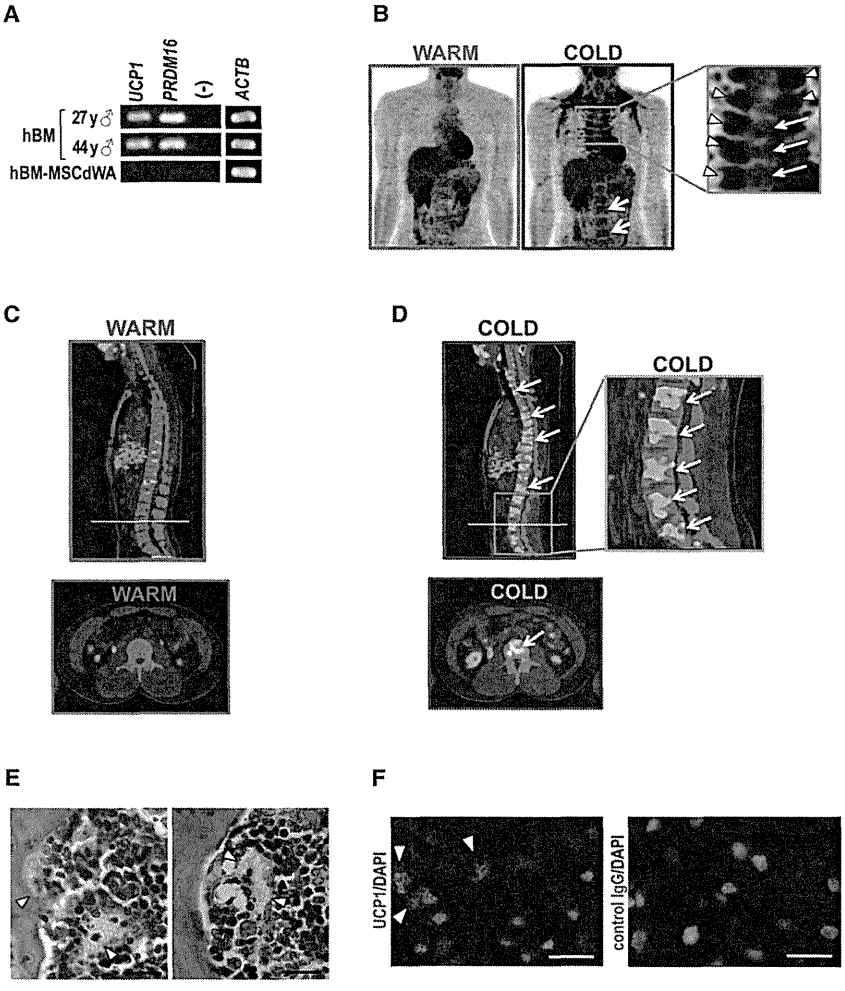

Figure 7. Examinations on BM-BAT

(A) Expression of *PRDM16* and *UCP1* in BM RNA samples of 27-year-old and 41-year-old males and human BM-derived hMSCdWA (hBM-MCdWA).

(B) ^{18}F-FDG-PET/CT. Typical results of the frontal images under warm and cold conditions were shown. Arrows indicate ^{18}F-FDG uptake into vertebrae per se, and arrowheads indicate ^{18}F-FDG uptake into classical paravertebral BA.

(C and D) Shown are sagittal and axial section images of ^{18}F-FDG-PET/CT under warm (C) and cold conditions (D). Arrows indicate the ^{18}F-FDG uptake into vertebral BM.

(E and F) Thoracic vertebra of 3-week-old ICR mice was subjected to HE staining (E) or UCP1 immunostaining (FF). Arrowheads indicate the existence of BA.

were measured by Accutrend Plus (F. Hoffmann-La Roche, Ltd., Basel, Switzerland). For oral fat tolerance tests, ICR mice were subcutaneously transplanted with immature hPSC or hPSCdBA and kept abstained from feed. After 16 hr, isoproterenol (15 μmol/kg) was administrated. After another 2 hr, 200 μl of olive oil was orally administrated, and blood TG levels were measured every 2 hr.

Assessment of Glucose Metabolism

The 1 × 10^6 of hESCdBA or hMSCdWA was transplanted to 6- or 10-week-old male ICR mice, which were kept abstained from feed. After 16 hr, isoproterenol (30 μmol/kg) was administrated. After another 4 hr, 2 g/kg of glucose (041-00595, Wako Pure Chemical Industries, Ltd., Osaka, Japan) was orally administrated. Blood sample were taken after 0, 15, 30, and 60 min. Blood glucose concentrations were measured by Accutrend Plus, and plasma insulin concentrations were measured by mouse insulin ELISA kit (Morinaga Institute of Biological Science, Inc., Yokohama, Japan).

Oxygen Consumption Analyses

The adherent culture step of BA differentiation was performed on special 96-well plates (Seahorse Bioscience Inc., Billerica, MA) precoated by 0.1% gelatin by seeding 30 spheres per well. Oxygen consumption was analyzed by Extracellular Flux Analyzer XF96 (Seahorse Bioscience Inc.) according to the manufacturer's guidance.

Calorigenic Analyses

The 1 × 10^6 of hPSCdBA or immature hPSCs were suspended in 100 μl saline and subcutaneously transplanted into 5-week-old male ICR mice After 24 hr, 30 μmol/kg of isoproterenol (12760, Sigma Chemical Co.) was administrated from the tail vein. After another 4 hr, mice were anesthetized, and dermal temperature was measured by Thermo GEAR G120/G100 (NEC Avio Infrared Technologies Co., Ltd, Tokyo, Japan). All animal care procedures involved in calorigenic analyses, assessment of lipid and metabolism, and hematopoietic stromal assays were approved by the Animal Care and Use Committee of the Research Institute, National Center for Global Health and Medicine (NCGM), and complied with the procedures of the Guide for the Care and Use of Laboratory Animals of NCGM.

Assessment of Lipid Metabolism

Six-week-old male CR mice were subcutaneously transplanted with 1 × 10^6 of immature hESC, hESCdBA, or hMC-derived WA suspended in 100 μl saline and kept abstained from feed. After 16 hr, isoproterenol (30 μmol/kg) was administrated. After another 2 hr, blood samples were taken, and TG concentrations

Hematopoietic Stromal Assays

The human cord blood CD34$^+$ cells were cultured on hPSCdBA layers without recombinant cytokines in RPMI1640 medium supplemented with 10% fetal calf serum. Floating cells were collected after 7 days, and 2 × 10^5 cells were transplanted into tibial bone marrow of NOG mice. After 6, 8, and 12 weeks, cells were collected from contralateral femoral bone marrow and spleen and subjected to cytometry using an anti-human CD45-FITC (clone J33) (Beckman Coulter Inc.) and anti-human CD33-PE antibody (clone WM53) (BD Biosciences, San Jose, CA). For control, cord blood CD34$^+$ cells were directly transplanted without coculture. For myelosuppression recovery assays, 100 mg/kg of 5-FU was intraperitoneally administrated. From day 3 to day 6, 30 μmol/kg of isoproterenol was administrated from tail vein. At day 7, bone marrow cells were collected from femoral bones and analyzed.

^{18}F-FDG-PET/CT Examinations

After careful instruction regarding the study and informed consent to participants, PET/CT examinations of healthy young volunteers (24.8 ± 5.8 years of age, n = 20) were performed. The protocol was approved by the institutional review boards of Tenshi College. Standardized uptake value (SUV) was measured by an expert as described in the Supplemental Experimental Procedures. Data are reported as means ± SEM. Statistics analyses were performed using SPSS software, version 18 (International Business Machines

Corp, New York), as described in the Supplemental Experimental Procedures. P values are considered to be statistically significant if <0.05.

SUPPLEMENTAL INFORMATION

Supplemental Information includes seven figures, Supplemental Experimental Procedures, and Supplemental References and can be found with this article online at http://dx.doi.org/10.1016/j.cmet.2012.08.001.

ACKNOWLEDGMENTS

This work was supported by Grant-in-Aid from Ministry of Health, Labour and Welfare of Japan (KHD1017) and by Japan Science and Technology Agency (AS 2321379G). We thank Mr. Kameya at LSI Sapporo Clinic for technical assistance for PET-CT examinations and Mr. Obara at LSI Sapporo Clinic for general assistance.

Received: March 17, 2012
Revised: June 30, 2012
Accepted: August 1, 2012
Published online: September 4, 2012

REFERENCES

Ahfeldt, T., Schinzel, R.T., Lee, Y.K., Hendrickson, D., Kaplan, A., Lum, D.H., Camahort, R., Xia, F., Shay, J., Rhee, E.P., et al. (2012). Programming human pluripotent stem cells into white and brown adipocytes. Nat. Cell Biol. *14*, 209–219.

Arai, F., and Suda, T. (2007). Maintenance of quiescent hematopoietic stem cells in the osteoblastic niche. Ann. N Y Acad. Sci. *1106*, 41–53.

Asano, A., Morimatsu, M., Nikami, H., Yoshida, T., and Saito, M. (1997). Adrenergic activation of vascular endothelial growth factor mRNA expression in rat brown adipose tissue: implication in cold-induced angiogenesis. Biochem. J. *328*, 179–183.

Bartelt, A., Bruns, O.T., Reimer, R., Hohenberg, H., Ittrich, H., Peldschus, K., Kaul, M.G., Tromsdorf, U.I., Weller, H., Waurisch, C., et al. (2011). Brown adipose tissue activity controls triglyceride clearance. Nat. Med. *17*, 200–205.

Braun, T., and Arnold, H.H. (1996). Myf-5 and myoD genes are activated in distinct mesenchymal stem cells and determine different skeletal muscle cell lineages. EMBO J. *15*, 310–318.

Calo, E., Quintero-Estades, J.A., Danielian, P.S., Nedelcu, S., Berman, S.D., and Lees, J.A. (2010). Rb regulates fate choice and lineage commitment in vivo. Nature *466*, 1110–1114.

Cossu, G., Kelly, R., Tajbakhsh, S., Di Donna, S., Vivarelli, E., and Buckingham, M. (1996). Activation of different myogenic pathways: myf-5 is induced by the neural tube and MyoD by the dorsal ectoderm in mouse paraxial mesoderm. Development *122*, 429–437.

Crisan, M., Yap, S., Casteilla, L., Chen, C.W., Corselli, M., Park, T.S., Andriolo, G., Sun, B., Zheng, B., Zhang, L., et al. (2008). A perivascular origin for mesenchymal stem cells in multiple human organs. Cell Stem Cell *3*, 301–313.

Cypess, A.M., Lehman, S., Williams, G., Tal, I., Rodman, D., Goldfine, A.B., Kuo, F.C., Palmer, E.L., Tseng, Y.H., Doria, A., et al. (2009). Identification and importance of brown adipose tissue in adult humans. N. Engl. J. Med. *360*, 1509–1517.

Dexter, T.M., Allen, T.D., and Lajtha, L.G. (1977). Conditions controlling the proliferation of haemopoietic stem cells in vitro. J. Cell. Physiol. *91*, 335–344.

Elabd, C., Chiellini, C., Carmona, M., Galitzky, J., Cochet, O., Petersen, R., Pénicaud, L., Kristiansen, K., Bouloumié, A., Casteilla, L., et al. (2009). Human multipotent adipose-derived stem cells differentiate into functional brown adipocytes. Stem Cells *27*, 2753–2760.

Enerbäck, S., Jacobsson, A., Simpson, E.M., Guerra, C., Yamashita, H., Harper, M.E., and Kozak, L.P. (1997). Mice lacking mitochondrial uncoupling protein are cold-sensitive but not obese. Nature *387*, 90–94.

Feldmann, H.M., Golozoubova, V., Cannon, B., and Nedergaard, J. (2009). UCP1 ablation induces obesity and abolishes diet-induced thermogenesis in mice exempt from thermal stress by living at thermoneutrality. Cell Metab. *9*, 203–209.

Gimble, J.M., Dorheim, M.A., Cheng, Q., Medina, K., Wang, C.S., Jones, R., Koren, E., Pietrangeli, C., and Kincade, P.W. (1990). Adipogenesis in a murine bone marrow stromal cell line capable of supporting B lineage lymphocyte growth and proliferation: biochemical and molecular characterization. Eur. J. Immunol. *20*, 379–387.

Gimble, J.M., Youkhana, K., Hua, X., Bass, H., Medina, K., Sullivan, M., Greenberger, J., and Wang, C.S. (1992). Adipogenesis in a myeloid supporting bone marrow stromal cell line. J. Cell. Biochem. *50*, 73–82.

Gupta, R.K., Mepani, R.J., Kleiner, S., Lo, J.C., Khandekar, M.J., Cohen, P., Frontini, A., Bhowmick, D.C., Ye, L., Cinti, S., et al. (2012). Zfp423 expression identifies committed preadipocytes and localizes to adipose endothelial and perivascular cells. Cell Metab. *15*, 230–239.

Hiroyama, T., Miharada, K., Aoki, N., Fujioka, T., Sudo, K., Danjo, I., Nagasawa, T., and Nakamura, Y. (2006). Long-lasting in vitro hematopoiesis derived from primate embryonic stem cells. Exp. Hematol. *34*, 760–769.

Hofer, M., Pospísil, M., Znojil, V., Holá, J., Vacek, A., and Streitová, D. (2007). Adenosine A(3) receptor agonist acts as a homeostatic regulator of bone marrow hematopoiesis. Biomed. Pharmacother. *61*, 356–359.

Ito, M., Hiramatsu, H., Kobayashi, K., Suzue, K., Kawahata, M., Hioki, K., Ueyama, Y., Koyanagi, Y., Sugamura, K., Tsuji, K., et al. (2002). NOD/SCID/gamma(c)(null) mouse: an excellent recipient mouse model for engraftment of human cells. Blood *100*, 3175–3182.

Jacene, H.A., Cohade, C.C., Zhang, Z., and Wahl, R.L. (2011). The relationship between patients' serum glucose levels and metabolically active brown adipose tissue detected by PET/CT. Mol. Imaging Biol. *13*, 1278–1283.

Jackson, D.M., Hambly, C., Trayhurn, P., and Speakman, J.R. (2001). Can non-shivering thermogenesis in brown adipose tissue following NA injection be quantified by changes in overlying surface temperatures using infrared thermography? J. Therm. Biol. *26*, 85–93.

Kiel, M.J., and Morrison, S.J. (2006). Maintaining hematopoietic stem cells in the vascular niche. Immunity *25*, 862–864.

Kontani, Y., Wang, Y., Kimura, K., Inokuma, K.I., Saito, M., Suzuki-Miura, T., Wang, Z., Sato, Y., Mori, N., and Yamashita, H. (2005). UCP1 deficiency increases susceptibility to diet-induced obesity with age. Aging Cell *4*, 147–155.

Krings, A., Rahman, S., Huang, S., Lu, Y., Czernik, P.J., and Lecka-Czernik, B. (2012). Bone marrow fat has brown adipose tissue characteristics, which are attenuated with aging and diabetes. Bone *50*, 546–552.

Laharrague, P., Fontanilles, A.M., Tkaczuk, J., Corberand, J.X., Pénicaud, L., and Casteilla, L. (2000). Inflammatory/haematopoietic cytokine production by human bone marrow adipocytes. Eur. Cytokine Netw. *11*, 634–639.

Motyl, K.J., and Rosen, C.J. (2011). Temperatures rising: brown fat and bone. Discov. Med. *11*, 179–185.

Nagasawa, T. (2007). The chemokine CXCL12 and regulation of HSC and B lymphocyte development in the bone marrow niche. Adv. Exp. Med. Biol. *602*, 69–75.

Nakahara, M., Nakamura, N., Matsuyama, S., Yogiashi, Y., Yasuda, K., Kondo, Y., Yuo, A., and Saeki, K. (2009). High-efficiency production of subculturable vascular endothelial cells from feeder-free human embryonic stem cells without cell-sorting technique. Cloning Stem Cells *11*, 509–522.

Naveiras, O., Nardi, V., Wenzel, P.L., Hauschka, P.V., Fahey, F., and Daley, G.Q. (2009). Bone-marrow adipocytes as negative regulators of the haematopoietic microenvironment. Nature *460*, 259–263.

Ookura, N., Fujimori, Y., Nishioka, K., Kai, S., Hara, H., and Ogawa, H. (2007). Adipocyte differentiation of human marrow mesenchymal stem cells reduces the supporting capacity for hematopoietic progenitors but not for severe combined immunodeficiency repopulating cells. Int. J. Mol. Med. *19*, 387–392.

Osafune, K., Caron, L., Borowiak, M., Martinez, R.J., Fitz-Gerald, C.S., Sato, Y., Cowan, C.A., Chien, K.R., and Melton, D.A. (2008). Marked differences in differentiation propensity among human embryonic stem cell lines. Nat. Biotechnol. *26*, 313–315.

Ouellet, V., Routhier-Labadie, A., Bellemare, W., Lakhal-Chaieb, L., Turcotte, E., Carpentier, A.C., and Richard, D. (2011). Outdoor temperature, age, sex, body mass index, and diabetic status determine the prevalence, mass, and glucose-uptake activity of 18F-FDG-detected BAT in humans. J. Clin. Endocrinol. Metab. *96*, 192–199.

Petrovic, N., Walden, T.B., Shabalina, I.G., Timmons, J.A., Cannon, B., and Nedergaard, J. (2010). Chronic peroxisome proliferator-activated receptor gamma (PPARgamma) activation of epididymally derived white adipocyte cultures reveals a population of thermogenically competent, UCP1-containing adipocytes molecularly distinct from classic brown adipocytes. J. Biol. Chem. *285*, 7153–7164.

Reznikoff, C.A., Brankow, D.W., and Heidelberger, C. (1973). Establishment and characterization of a cloned line of C3H mouse embryo cells sensitive to postconfluence inhibition of division. Cancer Res. *33*, 3231–3238.

Saeki, K., Yuo, A., Okuma, E., Yazaki, Y., Susin, S.A., Kroemer, G., and Takaku, F. (2000). Bcl-2 down-regulation causes autophagy in a caspase-independent manner in human leukemic HL60 cells. Cell Death Differ. *7*, 1263–1269.

Saito, M., Okamatsu-Ogura, Y., Matsushita, M., Watanabe, K., Yoneshiro, T., Nio-Kobayashi, J., Iwanaga, T., Miyagawa, M., Kameya, T., Nakada, K., et al. (2009). High incidence of metabolically active brown adipose tissue in healthy adult humans: effects of cold exposure and adiposity. Diabetes *58*, 1526–1531.

Sakurai, H., Era, T., Jakt, L.M., Okada, M., Nakai, S., Nishikawa, S., and Nishikawa, S. (2006). In vitro modeling of paraxial and lateral mesoderm differentiation reveals early reversibility. Stem Cells *24*, 575–586.

Seale, P., Kajimura, S., Yang, W., Chin, S., Rohas, L.M., Uldry, M., Tavernier, G., Langin, D., and Spiegelman, B.M. (2007). Transcriptional control of brown fat determination by PRDM16. Cell Metab. *6*, 38–54.

Seale, P., Bjork, B., Yang, W., Kajimura, S., Chin, S., Kuang, S., Scimè, A., Devarakonda, S., Conroe, H.M., Erdjument-Bromage, H., et al. (2008). PRDM16 controls a brown fat/skeletal muscle switch. Nature *454*, 961–967.

Sellayah, D., Bharaj, P., and Sikder, D. (2011). Orexin is required for brown adipose tissue development, differentiation, and function. Cell Metab. *14*, 478–490.

Suemori, H., Yasuchika, K., Hasegawa, K., Fujioka, T., Tsuneyoshi, N., and Nakatsuji, N. (2006). Efficient establishment of human embryonic stem cell lines and long-term maintenance with stable karyotype by enzymatic bulk passage. Biochem. Biophys. Res. Commun. *345*, 926–932.

Sun, L., Xie, H., Mori, M.A., Alexander, R., Yuan, B., Hattangadi, S.M., Liu, Q., Kahn, C.R., and Lodish, H.F. (2011). Mir193b-365 is essential for brown fat differentiation. Nat. Cell Biol. *13*, 958–965.

Takayama, N., Nishikii, H., Usui, J., Tsukui, H., Sawaguchi, A., Hiroyama, T., Eto, K., and Nakauchi, H. (2008). Generation of functional platelets from human embryonic stem cells in vitro via ES-sacs, VEGF-promoted structures that concentrate hematopoietic progenitors. Blood *111*, 5298–5306.

Tanaka, Y., and Inoue, T. (1976). Fatty marrow in the vertebrae. A parameter for hematopoietic activity in the aged. J. Gerontol. *31*, 527–532.

Thorns, C., Schardt, C., Katenkamp, D., Kähler, C., Merz, H., and Feller, A.C. (2008). Hibernoma-like brown fat in the bone marrow: report of a unique case. Virchows Arch. *452*, 343–345.

Timmons, J.A., Wennmalm, K., Larsson, O., Walden, T.B., Lassmann, T., Petrovic, N., Hamilton, D.L., Gimeno, R.E., Wahlestedt, C., Baar, K., et al. (2007). Myogenic gene expression signature establishes that brown and white adipocytes originate from distinct cell lineages. Proc. Natl. Acad. Sci. USA *104*, 4401–4406.

Tonello, C., Giordano, A., Cozzi, V., Cinti, S., Stock, M.J., Carruba, M.O., and Nisoli, E. (1999). Role of sympathetic activity in controlling the expression of vascular endothelial growth factor in brown fat cells of lean and genetically obese rats. FEBS Lett. *442*, 167–172.

Tran, K.V., Gealekman, O., Frontini, A., Zingaretti, M.C., Morroni, M., Giordano, A., Smorlesi, A., Perugini, J., De Matteis, R., Sbarbati, A., et al. (2012). The vascular endothelium of the adipose tissue gives rise to both white and brown fat cells. Cell Metab. *15*, 222–229.

Tseng, Y.H., Kokkotou, E., Schulz, T.J., Huang, T.L., Winnay, J.N., Taniguchi, C.M., Tran, T.T., Suzuki, R., Espinoza, D.O., Yamamoto, Y., et al. (2008). New role of bone morphogenetic protein 7 in brown adipogenesis and energy expenditure. Nature *454*, 1000–1004.

van Marken Lichtenbelt, W.D., Vanhommerig, J.W., Smulders, N.M., Drossaerts, J.M., Kemerink, G.J., Bouvy, N.D., Schrauwen, P., and Teule, G.J. (2009). Cold-activated brown adipose tissue in healthy men. N. Engl. J. Med. *360*, 1500–1508.

Virtanen, K.A., Lidell, M.E., Orava, J., Heglind, M., Westergren, R., Niemi, T., Taittonen, M., Laine, J., Savisto, N.J., Enerbäck, S., and Nuutila, P. (2009). Functional brown adipose tissue in healthy adults. N. Engl. J. Med. *360*, 1518–1525.

Yoneshiro, T., Aita, S., Matsushita, M., Okamatsu-Ogura, Y., Kameya, T., Kawai, Y., Miyagawa, M., Tsujisaki, M., and Saito, M. (2011). Age-related decrease in cold-activated brown adipose tissue and accumulation of body fat in healthy humans. Obesity (Silver Spring) *19*, 1755–1760.

Efficient Generation of Functional Hepatocytes From Human Embryonic Stem Cells and Induced Pluripotent Stem Cells by HNF4α Transduction

Kazuo Takayama[1,2], Mitsuru Inamura[1,2], Kenji Kawabata[2,3], Kazufumi Katayama[1], Maiko Higuchi[2], Katsuhisa Tashiro[2], Aki Nonaka[2], Fuminori Sakurai[1], Takao Hayakawa[4,5], Miho Kusuda Furue[6,7] and Hiroyuki Mizuguchi[1,2,8]

[1]Laboratory of Biochemistry and Molecular Biology, Graduate School of Pharmaceutical Sciences, Osaka University, Osaka, Japan; [2]Laboratory of Stem Cell Regulation, National Institute of Biomedical Innovation, Osaka, Japan; [3]Laboratory of Biomedical Innovation, Graduate School of Pharmaceutical Sciences, Osaka University, Osaka, Japan; [4]Pharmaceutics and Medical Devices Agency, Tokyo, Japan; [5]Pharmaceutical Research and Technology Institute, Kinki University, Osaka, Japan; [6]JCRB Cell Bank, Division of Bioresources, National Institute of Biomedical Innovation, Osaka, Japan; [7]Laboratory of Cell Processing, Institute for Frontier Medical Sciences, Kyoto University, Kyoto, Japan; [8]The Center for Advanced Medical Engineering and Informatics, Osaka University, Osaka, Japan

Hepatocyte-like cells from human embryonic stem cells (ESCs) and induced pluripotent stem cells (iPSCs) are expected to be a useful source of cells drug discovery. Although we recently reported that hepatic commitment is promoted by transduction of SOX17 and HEX into human ESC- and iPSC-derived cells, these hepatocyte-like cells were not sufficiently mature for drug screening. To promote hepatic maturation, we utilized transduction of the hepatocyte nuclear factor 4α (HNF4α) gene, which is known as a master regulator of liver-specific gene expression. Adenovirus vector-mediated overexpression of HNF4α in hepatoblasts induced by SOX17 and HEX transduction led to upregulation of epithelial and mature hepatic markers such as cytochrome P450 (CYP) enzymes, and promoted hepatic maturation by activating the mesenchymal-to-epithelial transition (MET). Thus HNF4α might play an important role in the hepatic differentiation from human ESC-derived hepatoblasts by activating the MET. Furthermore, the hepatocyte like-cells could catalyze the toxication of several compounds. Our method would be a valuable tool for the efficient generation of functional hepatocytes derived from human ESCs and iPSCs, and the hepatocyte-like cells could be used for predicting drug toxicity.

Received 19 July 2011; accepted 28 September 2011; published online 8 November 2011. doi:10.1038/mt.2011.234

INTRODUCTION

Human embryonic stem cells (ESCs) and induced pluripotent stem cells (iPSCs) are able to replicate indefinitely and differentiate into most of the body's cell types.[1,2] They could provide an unlimited source of cells for various applications. Hepatocyte-like cells, which are differentiated from human ESCs and iPSCs, would be useful for basic research, regenerative medicine, and drug discovery.[3] In particular, it is expected that hepatocyte-like cells will be utilized as a tool for cytotoxicity screening in the early phase of pharmaceutical development. To catalyze the toxication of several compounds, hepatocyte-like cells need to be mature enough to exhibit hepatic functions, including high activity levels of the cytochrome P450 (CYP) enzymes. Because the present technology for the generation of hepatocyte-like cells from human ESCs and iPSCs, which is expected to be utilized for drug discovery, is not refined enough for this application, it is necessary to improve the efficiency of hepatic differentiation. Although conventional methods such as growth factor-mediated hepatic differentiation are useful to recapitulate liver development, they lead to only a heterogeneous hepatocyte population.[4–6] Recently, we showed that transcription factors are transiently transduced to promote hepatic differentiation in addition to the conventional differentiation method which uses only growth factors.[7] Ectopic expression of Sry-related HMG box 17 (SOX17) or hematopoietically expressed homeobox (HEX) by adenovirus (Ad) vectors in human ESC-derived mesendoderm or definitive endoderm (DE) cells markedly enhances the endoderm differentiation or hepatic commitment, respectively.[7,8] However, further hepatic maturation is required for drug screening.

The transcription factor hepatocyte nuclear factor 4α (HNF4α) is initially expressed in the developing hepatic diverticulum on E8.75,[9,10] and its expression is elevated as the liver develops. A previous loss-of-function study showed that HNF4α plays a critical role in liver development; conditional deletion of *HNF4α* in fetal hepatocytes results in the faint expression of many mature hepatic enzymes and the impairment of normal liver morphology.[11] The genome-scale chromatin immunoprecipitation assay showed that HNF4α binds to the promoters of nearly half of the genes expressed in the mouse liver,[12] including cell adhesion and junctional proteins,[13] which are important in

Correspondence: *Hiroyuki Mizuguchi, Laboratory of Biochemistry and Molecular Biology, Graduate School of Pharmaceutical Sciences, Osaka University, 1-6 Yamadaoka, Suita, Osaka 565-0871, Japan. E-mail: mizuguch@phs.osaka-u.ac.jp*

the hepatocyte epithelial structure.[14] In addition, HNF4α plays a critical role in hepatic differentiation and in a wide variety of liver functions, including lipid and glucose metabolism.[15,16] Although HNF4α could promote transdifferentiation into hepatic lineage from hematopoietic cells,[17] the function of HNF4α in hepatic differentiation from human ESCs and iPSCs remains unknown. A previous study showed that hepatic differentiation from mouse hepatic progenitor cells is promoted by HNF4α, although many of the hepatic markers that they examined were target genes of HNF4α.[18] They transplanted the HNF4α-overexpressed mouse hepatic progenitor cells to promote hepatic differentiation, but they did not examine the markers that relate to hepatic maturation such as CYP enzymes, conjugating enzymes, and hepatic transporters.

In this study, we examined the role of HNF4α in hepatic differentiation from human ESCs and iPSCs. The human ESC- and iPSC-derived hepatoblasts, which were efficiently generated by sequential transduction of SOX17 and HEX, were transduced with HNF4α-expressing Ad vector (Ad-HNF4α), and then the expression of hepatic markers of the hepatocyte-like cells were assessed. In addition, we examined whether or not the hepatocyte-like cells, which were generated by sequential transduction of SOX17, HEX, and HNF4α, were able to predict the toxicity of several compounds.

RESULTS

Stage-specific HNF4α transduction in hepatoblasts selectively promotes hepatic differentiation

The transcription factor HNF4α plays an important role in both liver generation[11] and hepatic differentiation from human ESCs and iPSCs (**Supplementary Figure S1**). We expected that hepatic differentiation could be accelerated by HNF4α transduction. To examine the effect of forced expression of HNF4α in the hepatic differentiation from human ESC- and iPSC-derived cells, we used a fiber-modified Ad vector.[19] Initially, we optimized the time period for Ad-HNF4α transduction. Human ESC (H9)-derived DE cells (day 6) (**Supplementary Figures S2** and **S3a**), hepatoblasts (day 9) (**Supplementary Figures S2** and **S3b**), or a heterogeneous population consisting of hepatoblasts, hepatocytes, and cholangiocytes (day 12) (**Supplementary Figures S2** and **S3c**) were transduced with Ad-HNF4α and then the Ad-HNF4α-transduced cells were cultured until day 20 of differentiation (**Figure 1**). We ascertained the expression of exogenous *HNF4α* in human ESC-derived hepatoblasts (day 9) transduced with Ad-HNF4α (**Supplementary Figure S4**). The transduction of Ad-HNF4α into human ESC-derived hepatoblasts (day 9) led to the highest expression levels of the hepatocyte markers *albumin* (*ALB*)[20] and *α-1-antitrypsin* (**Figure 1a**). In contrast, the expression levels of the cholangiocyte markers *cytokeratin 7* (*CK7*)[21] and *SOX9*[22] were

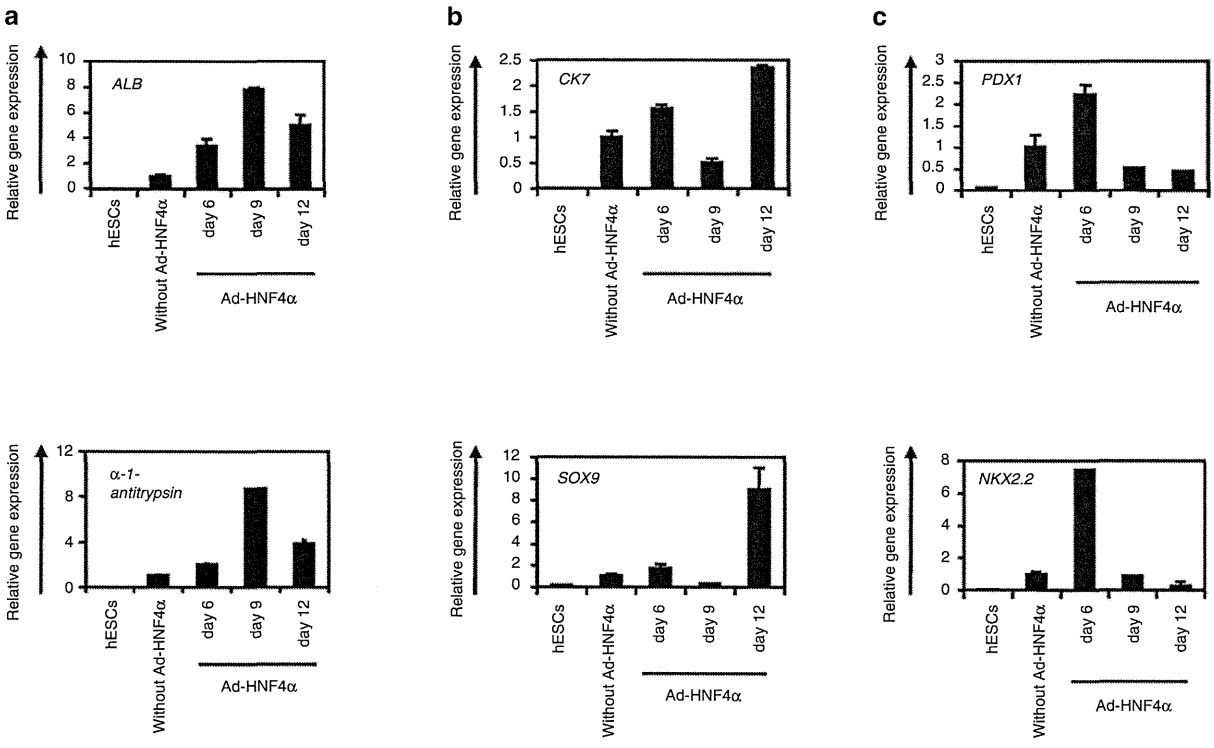

Figure 1 Transduction of HNF4α into hepatoblasts promotes hepatic differentiation. (**a–c**) The human ESC (H9)-derived cells, which were cultured for 6, 9, or 12 days according to the protocol described in **Figure 2a**, were transduced with 3,000 vector particles (VP)/cell of Ad-HNF4α for 1.5 hours and cultured until day 20. The gene expression levels of (**a**) hepatocyte markers (*ALB* and *α-1-antitrypsin*), (**b**) cholangiocyte markers (*CK7* and *SOX9*), and (**c**) pancreas markers (*PDX1* and *NKX2.2*) were examined by real-time RT-PCR on day 0 (human ESCs (hESCs)) or day 20 of differentiation. The horizontal axis represents the days when the cells were transduced with Ad-HNF4α. On the y-axis, the level of the cells without Ad-HNF4α transduction on day 20 was taken as 1.0. All data are represented as means ± SD ($n = 3$). ESC, embryonic stem cell; HNF4α, hepatocyte nuclear factor 4α; RT-PCR, reverse transcription-PCR.

downregulated in the cells transduced on day 9 as compared with nontransduced cells (**Figure 1b**). This might be because hepatic differentiation was selectively promoted and biliary differentiation was repressed by the transduction of HNF4α in hepatoblasts. The expression levels of the pancreas markers *PDX1*[23] and *NKX2.2*[24] did not make any change in the cells transduced on day 9 as compared with nontransduced cells (**Figure 1c**). Interestingly, the expression levels of the pancreas markers were upregulated, when Ad-HNF4α transduction was performed into DE cells (day 6) (**Figure 1c**). These results suggest that HNF4α might promote not only hepatic differentiation but also pancreatic differentiation, although the optimal stage of HNF4 transduction for the differentiation of each cell is different. We have confirmed that there was no difference between nontransduced cells and Ad-LacZ-transduced cells in the gene expression levels of all the markers investigated in **Figure 1a–c** (data not shown). We also confirmed that Ad vector-mediated gene expression in the human ESC-derived hepatoblasts (day 9) continued until day 14 and almost disappeared on day 18 (**Supplementary Figure S5**). These results indicated that the stage-specific HNF4α overexpression in human ESC-derived hepatoblasts (day 9) was essential for promoting efficient hepatic differentiation.

Transduction of HNF4α into human ESC- and iPSC-derived hepatoblasts efficiently promotes hepatic maturation

From the results of **Figure 1**, we decided to transduce hepatoblasts (day 9) with Ad-HNF4α. To determine whether hepatic maturation is promoted by Ad-HNF4α transduction, Ad-HNF4α-transduced cells were cultured until day 20 of differentiation according to the schematic protocol described in **Figure 2a**. After the hepatic maturation, the morphology of human ESCs was gradually changed into that of hepatocytes: polygonal with distinct round nuclei (day 20) (**Figure 2b**). Interestingly, a portion of the hepatocyte-like cells, which were ALB[20]-, CK18[21]-, CYP2D6-, and CYP3A4[25]-positive cells, had double nuclei, which was also observed in primary human hepatocytes (**Figure 2b,c**, and **Supplementary Figure S6**). We also examined the hepatic gene expression levels on day 20 of differentiation (**Figure 3a,b**). The gene expression analysis of *CYP1A2*, *CYP2C9*, *CYP2C19*, *CYP2D6*, *CYP3A4*, and *CYP7A1*[25] showed higher expression levels in all of Ad-SOX17-, Ad-HEX-, and Ad-HNF4α-transduced cells (three factors-transduced cells) as compared with those in both Ad-SOX17- and Ad-HEX-transduced cells (two factors-transduced cells) on day 20 (**Figure 3a**). The gene expression level of NADPH-CYP reductase

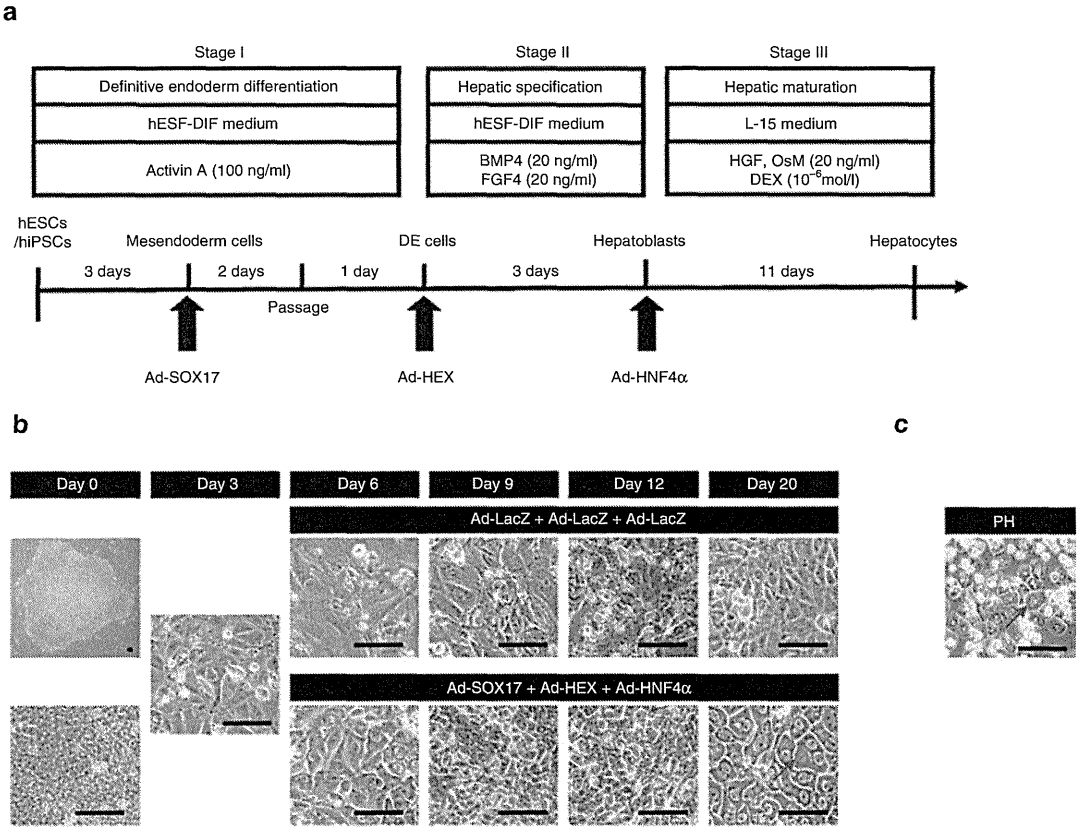

Figure 2 Hepatic differentiation of human ESCs and iPSCs transduced with three factors. (**a**) The procedure for differentiation of human ESCs and iPSCs into hepatocytes via DE cells and hepatoblasts is presented schematically. The hESF-DIF medium was supplemented with 10 μg/ml human recombinant insulin, 5 μg/ml human apotransferrin, 10 μmol/l 2-mercaptoethanol, 10 μmol/l ethanolamine, 10 μmol/l sodium selenite, and 0.5 mg/ml fatty-acid-free BSA. The L15 medium was supplemented with 8.3% tryptose phosphate broth, 8.3% FBS, 10 μmol/l hydrocortisone 21-hemisuccinate, 1 μmol/l insulin, and 25 mmol/l $NaHCO_3$. (**b**) Sequential morphological changes (day 0–20) of human ESCs (H9) differentiated into hepatocytes via DE cells and hepatoblasts are shown. Red arrow shows the cells that have double nuclei. (**c**) The morphology of primary human hepatocytes is shown. Bar represents 50 μm. BSA, bovine serum albumin; DE, definitive endoderm; ESC, embryonic stem cell; iPSC, induced pluripotent stem cell.

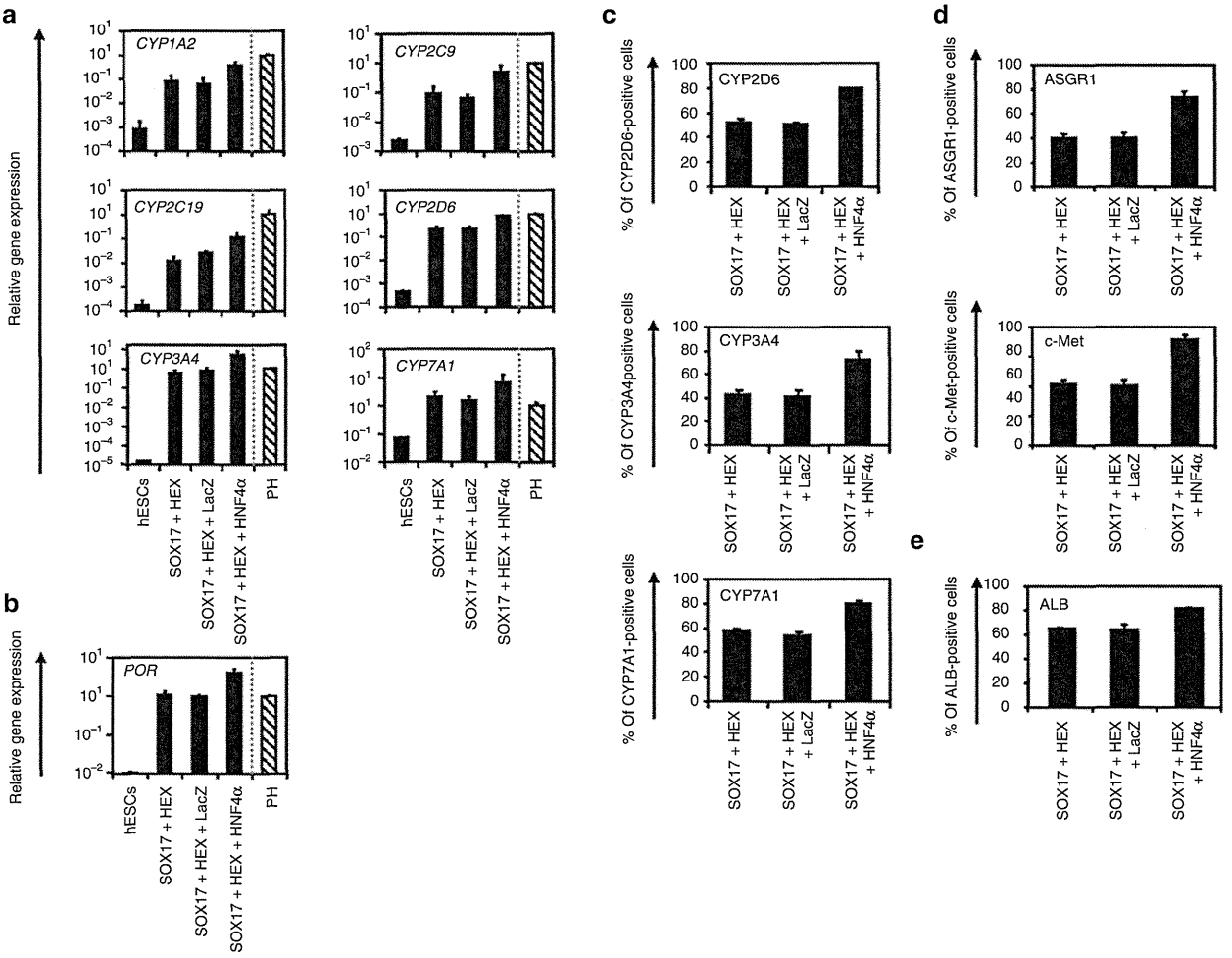

Figure 3 Transduction of HNF4α promotes hepatic maturation from human ESCs and iPSCs. (**a**,**b**) The human ESCs were differentiated into hepatocytes according to the protocol described in **Figure 2a**. On day 20 of differentiation, the gene expression levels of (**a**) CYP enzymes (*CYP1A2*, *CYP2C9*, *CYP2C19*, *CYP2D6*, *CYP3A4*, and *CYP7A1*) and (**b**) *POR* were examined by real-time RT-PCR in undifferentiated human ESCs (hESCs), the hepatocyte-like cells, and primary human hepatocytes (PH, hatched bar). On the y-axis, the expression level of primary human hepatocytes, which were cultured for 48 hours after the cells were plated, was taken as 1.0. (**c**–**e**) The hepatocyte-like cells (day 20) were subjected to immunostaining with (**c**) anti-drug-metabolizing enzymes (CYP2D6, CYP3A4, and CYP7A1), (**d**) anti-hepatic surface protein (ASGR1 and c-Met), and (**e**) anti-ALB antibodies, and then the percentage of antigen-positive cells was examined by flow cytometry on day 20 of differentiation. All data are represented as means ± SD (n = 3). ESC, embryonic stem cell; HNF4α, hepatocyte nuclear factor 4α; iPSC, induced pluripotent stem cell.

(POR)[26], which is required for the normal function of CYPs, was also higher in the three factors-transduced cells (**Figure 3b**). The gene expression analysis of ALB, α-1-antitrypsin (α-1-AT), transthyretin, hepatic conjugating enzymes, hepatic transporters, and hepatic transcription factors also showed higher expression levels in the three factors-transduced cells (**Supplementary Figures S7** and **S8**). Moreover, the gene expression levels of these hepatic markers of three factor-transduced cells were similar to those of primary human hepatocytes, although the levels depended on the type of gene (**Figure 3a,b**, and **Supplementary Figures S7** and **S8**). To confirm that similar results could be obtained with human iPSCs, we used three human iPS cell lines (201B7, Dotcom, and Tic). The gene expression of hepatic markers in human ESC- and iPSC-derived hepatocytes were analyzed by real-time reverse transcription-PCR on day 20 of differentiation. Three human iPS cell lines as well as human ESCs also effectively differentiated into hepatocytes in response to transduction of the three factors (**Supplementary Figure S9**). Interestingly, we observed differences in the hepatic maturation efficiency among the three human iPS cell lines. That is, two of the human iPS cell lines (Tic and Dotcom) were more committed to the hepatic lineage than another human iPS cell line (201B7). Because almost homogeneous hepatocyte-like cells would be more useful in basic research, regenerative medicine, and drug discovery, we also examined whether our novel methods for hepatic maturation could generate a homogeneous hepatocyte population by flow cytometry analysis (**Figure 3c–e**). The percentages of CYP2D6-, CYP3A4-, and CYP7A1-positive cells were ~80% in the three factors-transduced cells, while they were ~50% in the two factors-transduced cells (**Figure 3c**). The percentages of hepatic surface antigen (asialoglycoprotein receptor 1 (ASGR1] and met proto-oncogene (c-Met))-positive cells (**Figure 3d**) and ALB-positive cells (**Figure 3e**) were also ~80% in the three factors-transduced cells. These results indicated that a nearly homogeneous population was obtained by our differentiation protocol

using the transduction of three functional genes (SOX17, HEX, and HNF4α).

The three factors-transduced cells have characteristics of functional hepatocytes

The hepatic functions of the hepatocyte-like cells, such as the uptake of low-density lipoprotein (LDL) and CYP enzymes activity, of the hepatocyte-like cells were examined on day 20 of differentiation. Approximately 87% of the three factors-transduced cells uptook LDL in the medium, whereas only 44% of the two factors-transduced cells did so (**Figure 4a**). The activities of CYP enzymes of the hepatocyte-like cells were measured according to the metabolism of the CYP3A4, CYP2C9, or CYP1A2 substrates (**Figure 4b**). The metabolites were detected in the three factors-transduced cells and their activities were higher than those of the two factors-transduced cells (dimethyl sulfoxide (DMSO) column). We further tested the induction of CYP3A4, CYP2C9, and CYP1A2 by chemical stimulation, since CYP3A4, CYP2C9, and CYP1A2 are the important prevalent CYP isozymes in the liver and are involved in the metabolism of a significant proportion of the currently available commercial drugs (rifampicin or omeprazole column). It is well known that CYP3A4 and CYP2C9 can be induced by rifampicin, whereas CYP1A2 can be induced by omeprazole. The hepatocyte-like cells were treated with either of these. Although undifferentiated human ESCs responsed to neither rifampicin nor omeprazole (data not shown), the hepatocyte-like cells produced more metabolites in response to chemical stimulation as well as primary hepatocytes (**Figure 4b**). The activity levels of the hepatocyte-like cells as compared with those of primary human hepatocytes depended on the types of CYP; the CYP3A4 activity of the hepatocyte-like cells was similar to that of primary human hepatocytes, whereas the CYP2C9 and CYP1A2 activities of the hepatocyte-like cells were slightly lower than those of primary human hepatocytes (**Figure 3a**). These results indicated that high levels of functional CYP enzymes were detectable in the hepatocyte-like cells.

The metabolism of diverse compounds involving uptake, conjugation, and the subsequent release of the compounds is an important function of hepatocytes. Uptake and release of Indocyanine green (ICG) can often be used to identify hepatocytes in ESC differentiation models.[27] To investigate this function in our hepatocyte-like cells, we compared this ability of the three factors-transduced cells with that of the two factors-transduced cells on day 20 of differentiation (**Figure 4c**). The three factors-transduced cells had more ability to uptake ICG and to excrete ICG by culturing without ICG for 6 hours. We also examined whether the hepatocyte-like cells could store glycogen, a characteristic of functional hepatocytes (**Figure 4d**). On day 20 of differentiation, the three factors-transduced cells and the two factors-transduced cells were stained for cytoplasmic glycogen using the Periodic Acid-Schiff staining procedure. The three factors-transduced cells exhibited more abundant storage of glycogen than the two-factors-transduced cells. These results showed that abundant hepatic functions, such as uptake and excretion of ICG and storage of glycogen, were obtained by the transduction of three factors.

Many adverse drug reactions are caused by the CYP-dependent activation of drugs into reactive metabolites.[28] In order to examine metabolism-mediated toxicity and to improve the safety of drug candidates, primary human hepatocytes are widely used.[28] Because primary human hepatocytes have quite different characteristics among distinct lots and because it is difficult to purchase large amounts of primary human hepatocytes that have the same characteristics, hepatocyte-like cells are expected to be used for this purpose. To examine whether our hepatocyte-like cells could be used to predict metabolism-mediated toxicity, the hepatocyte-like cells were incubated with four substrates (troglitazone, acetaminophen, cyclophosphamide, and carbamazepine), which are known to generate toxic metabolites by CYP enzymes, and then the cell viability was measured (**Figure 4e**). The cell viability of the two factors plus Ad-LacZ-tansduced cells were higher than that of the three factors-transduced cells at each different concentration of four test compounds. These results indicated that the three factors-transduced cells could more efficiently metabolize the test compounds and thereby induce higher toxicity than either the two factors-transduced cells or undifferentiated human ESCs. The cell viability of the three factors-transduced cells was slightly higher than that of primary human hepatocytes.

HNF4α promotes hepatic maturation by activating mesenchymal-to-epithelial transition

HNF4α is known as a dominant regulator of the epithelial phenotype because its ectopic expression in fibroblasts (such as NIH 3T3 cells) induces mesenchymal-to-epithelial transition (MET)[11], although it is not known whether HNF4α can promote MET in hepatic differentiation. Therefore, we examined whether HNF4α transduction promotes hepatic maturation from hepatoblasts by activating MET. To clarify whether MET is activated by HNF4α transduction, the human ESC-derived hepatoblasts (day 9) were transduced with Ad-LacZ or Ad-HNF4α, and the resulting phenotype was analyzed on day 12 of differentiation (**Figure 5**). This time, we confirmed that HNF4α transduction decreased the population of N-cadherin (hepatoblast marker)-positive cells,[29] whereas it increased that of ALB (hepatocyte marker)-positive cells (**Figure 5a**). The number of CK7 (cholangiocyte marker)-positive population did not change (**Figure 5a**). To investigate whether these results were attributable to MET, the alteration of the expression of several mesenchymal and epithelial markers was examined (**Figure 5b**). The human ESC-derived hepatoblasts (day 9) were almost homogeneously N-cadherin[30] (mesenchymal marker)-positive and E-cadherin[11] (epithelial marker)-negative, demonstrating that human ESC-derived hepatoblasts have mesenchymal characteristics (**Figure 5a,b**). After HNF4α transduction, the number of E-cadherin-positive cells was increased and reached ~90% on day 20, whereas that of N-cadherin-positive cells was decreased and was less than 5% on day 20 (**Supplementary Figure S10**). These results indicated that MET was promoted by HNF4α transduction in hepatic differentiation from hepatoblasts. Interestingly, the number of growing cells was decreased by HNF4α transduction (**Figure 5c**), and the cell growth was delayed by HNF4α transduction (**Supplementary Figure S11**). This decrease in the number of growing cells might have been because the differentiation was promoted by HNF4α transduction. We also confirmed that MET was promoted by HNF4α transduction in the gene expression levels (**Figure 5d**).

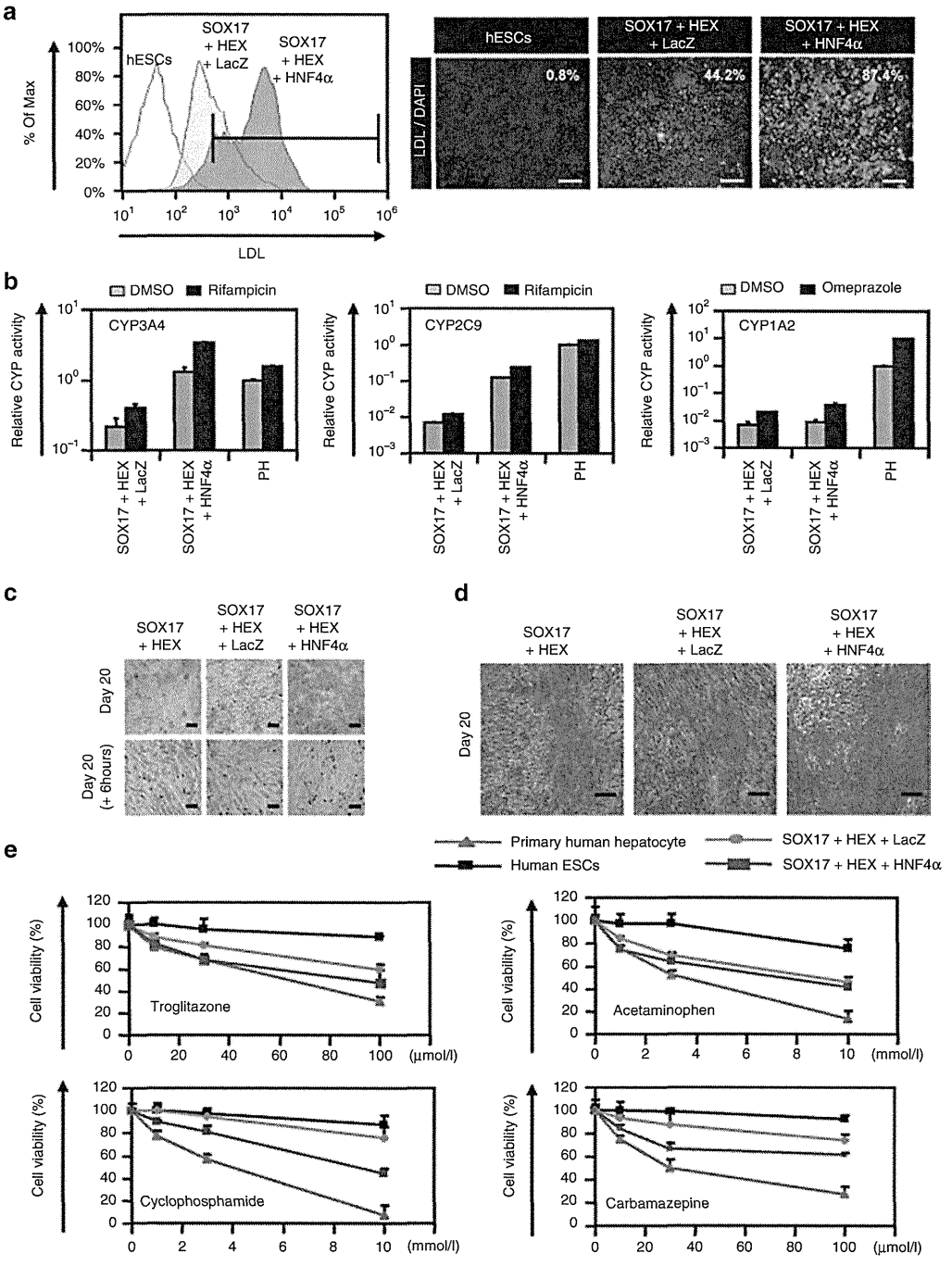

Figure 4 Transduction of the three factors enhances hepatic functions. The human ESCs were differentiated into hepatoblasts and transduced with 3,000 VP/cell of Ad-LacZ or Ad-HNF4α for 1.5 hours and cultured until day 20 of differentiation according to the protocol described in **Figure 2a**. The hepatic functions of the two factors plus Ad-LacZ-transduced cells (SOX17+HEX+LacZ) and the three factors-transduced cells (SOX17+HEX+HNF4α) were compared. (**a**) Undifferentiated human ESCs (hESCs) and the hepatocyte-like cells (day 20) were cultured with medium containing Alexa-Flour 488-labeled LDL (green) for 1 hour, and immunohistochemistry and flow cytometry analysis were performed. The percentage of LDL-positive cells was measured by flow cytometry. Nuclei were counterstained with DAPI (blue). The bar represents 100 μm. (**b**) Induction of CYP3A4 (left), CYP2C9 (middle), or CYP1A2 (right) by DMSO (gray bar), rifampicin (black bar), or omeprazole (black bar) in the hepatocyte-like cells (day 20) and primary human hepatocytes (PH), which were cultured for 48 hours after the cells were plated. On the y-axis, the activity of primary human hepatocytes that have been cultured with medium containing DMSO was taken as 1.0. (**c**) The hepatocyte-like cells (day 20) (upper column) were examined for their ability to take up Indocyanin Green (ICG) and release it 6 hours thereafter (lower column). (**d**) Glycogen storage of the hepatocyte-like cells (day 20) was assessed by Periodic Acid-Schiff (PAS) staining. PAS staining was performed on day 20 of differentiation. Glycogen storage is indicated by pink or dark red-purple cytoplasms. The bar represents 100 μm. (**e**) The cell viability of undifferentiated human ESCs (black), two factors plus Ad-LacZ-tansduced cells (green), the three factors-transduced cells (blue), and primary human hepatocytes (red) was assessed by Alamar Blue assay after 48 hours exposure to different concentrations of four test compounds (troglitazone, acetaminophen, cyclophosphamide, and carbamazepine). The cell viability is expressed as a percentage of cells treated with solvent only treat: 0.1% DMSO except for carbamazepine: 0.5% DMSO. All data are represented as means ± SD (n = 3). ESC, embryonic stem cell; DMSO, dimethyl sulfoxide; LDL, low-density lipoprotein.

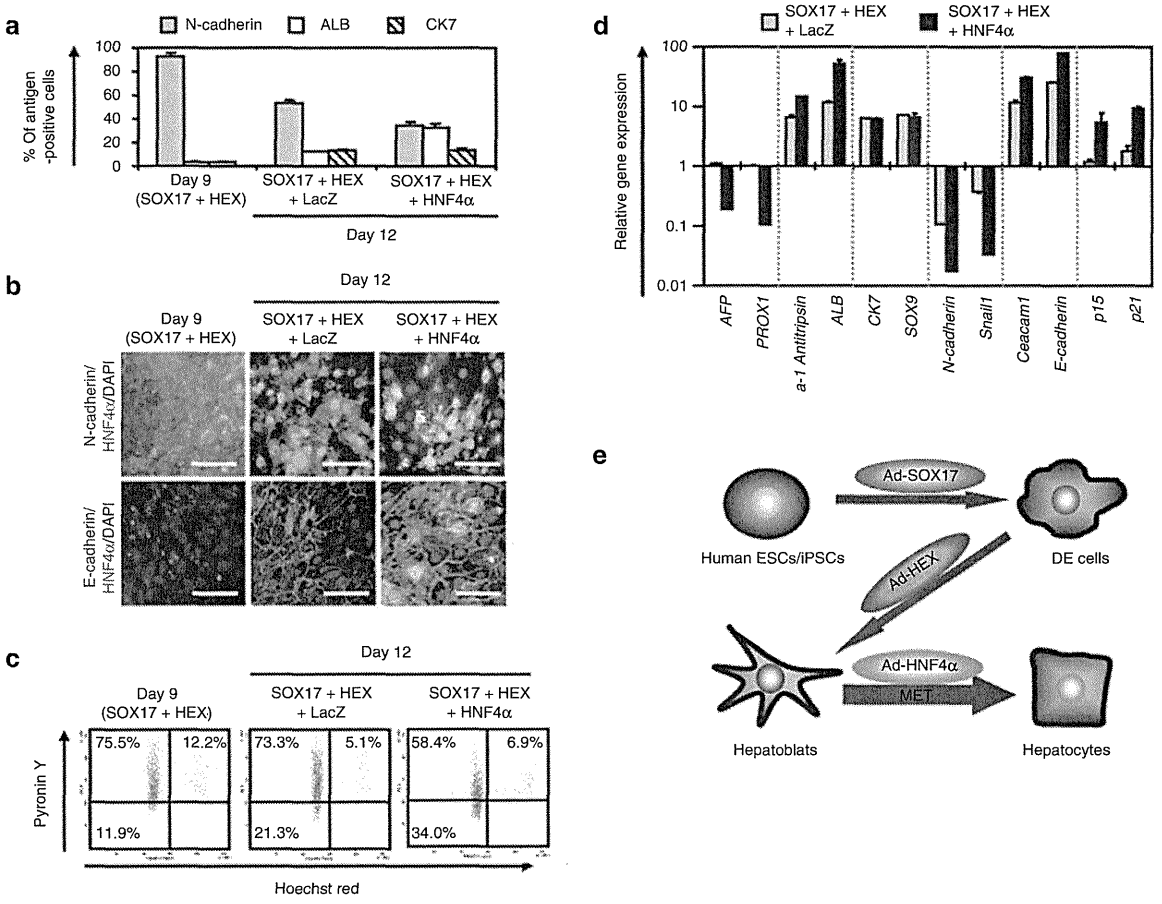

Figure 5 HNF4α promotes hepatic differentiation by activating MET. Human ESCs were differentiated into hepatoblasts according to the protocol described in **Figure 2a**, and then transduced with 3,000 VP/cell of Ad-LacZ or Ad-HNF4α for 1.5 hours, and finally cultured until day 12 of differentiation. (**a**) The hepatoblasts, two factors plus Ad-LacZ-transduced cells (SOX17+HEX+LacZ) (day 12), and the three factors-transduced cells (SOX17+HEX+HNF4α) (day 12) were subjected to immunostaining with anti-N-cadherin, ALB, or CK7 antibodies. The percentage of antigen-positive cells was measured by flow cytometry. (**b**) The cells were subjected to immunostaining with anti-N-cadherin (green), E-cadherin (green), or HNF4α (red) antibodies on day 9 or day 12 of differentiation. Nuclei were counterstained with DAPI (blue). The bar represents 50 μm. Similar results were obtained in two independent experiments. (**c**) The cell cycle was examined on day 9 or day 12 of differentiation. The cells were stained with Pyronin Y (y-axis) and Hoechst 33342 (x-axis) and then analyzed by flow cytometry. The growth fraction of cells is the population of actively dividing cells (G1/S/G2/M). (**d**) The expression levels of *AFP*, *PROX1*, *α-1-antitrypsin*, *ALB*, *CK7*, *SOX9*, *N-cadherin*, *Snail1*, *Ceacam1*, *E-cadherin*, *p15*, and *p21* were examined by real-time RT-PCR on day 9 or day 12 of differentiation. The expression level of hepatoblasts (day 9) was taken as 1.0. All data are represented as means ± SD ($n = 3$). (**e**) The model of efficient hepatic differentiation from human ESCs and iPSCs in this study is summarized. The human ESCs and iPSCs differentiate into hepatocytes via definitive endoderm and hepatoblasts. At each stage, the differentiation is promoted by stage-specific transduction of appropriate functional genes. In the last stage of hepatic differentiation, HNF4α transduction provokes hepatic maturation by activating MET. ESC, embryonic stem cell; HNF4α, hepatocyte nuclear factor 4α; iPSC, induced pluripotent stem cell; MET, mesenchymal-to-epithelial transition; RT-PCR, reverse transcription-PCR; VP, vector particle.

The gene expression levels of hepatocyte markers (*α-1-antitrypsin* and *ALB*)[20] and epithelial markers (*Ceacam1* and *E-cadherin*) were upregulated by HNF4α transduction. On the other hand, the gene expression levels of hepatoblast markers (*AFP* and *PROX1*)[31], mesenchymal markers (*N-cadherin* and *Snail*)[32], and cyclin dependent kinase inhibitor (*p15* and *p21*)[33] were downregulated by HNF4α transduction. HNF4α transduction did not change the expression levels of cholangiocyte markers (*CK7* and *SOX9*). We conclude that HNF4α promotes hepatic maturation by activating MET.

DISCUSSION

This study has two main purposes: the generation of functional hepatocytes from human ESCs and iPSCs for application to drug toxicity screening in the early phase of pharmaceutical development and; elucidation of the HNF4α function in hepatic maturation from human ESCs. We initially confirmed the importance of transcription factor HNF4α in hepatic differentiation from human ESCs by using a published data set of gene array analysis (**Supplementary Figure S1**).[34] We speculated that HNF4α transduction could enhance hepatic differentiation from human ESCs and iPSCs.

To generate functional hepatocytes from human ESCs and iPSCs and to elucidate the function of HNF4α in hepatic differentiation from human ESCs, we examined the stage-specific roles of HNF4α. We found that hepatoblast (day 9) stage-specific HNF4α transduction promoted hepatic differentiation (**Figure 1**). Because endogenous HNF4α is initially expressed in the hepatoblast,[9,10] our system might adequately reflect early embryogenesis. However, HNF4α transduction at an inappropriate stage (day 6 or day 12) promoted